Ontario

We are committed to providing accessible customer service.
If you need accessible formats or communications supports, please contact us.

Nous tenons à améliorer l'accessibilité des services à la clientèle.
Si vous avez besoin de formats accessibles ou d'aide à la communication, veuillez nous contacter.

REPORT ON A HELICOPTER-BORNE TIME DOMAIN ELECTROMAGNETIC AND MAGNETIC SURVEY AT DUBREILVILLE, ON

Project Name: **Goudreau Project**

Project Number: **2020-02-17**

Client: Manitou Gold Inc.

Contractor: BECI exploration consulting

Date Submitted: **October 1, 2020**

TABLE OF CONTENTS

FIGURES

TABLES

1.0 INTRODUCTION

1.1 CONTRACTOR

Balch Exploration Consulting Inc. (“BECI”, the “Contractor”) having its head office at 11500 Fifth Line, Rockwood, Ontario, Canada, N0B 2K0, has performed a helicopter time domain electromagnetic and magnetic survey using the AirTEM™ system developed by Triumph Instruments.

1.2 CLIENT

Manitou Gold Inc. (“Manitou”, or the “Client”) having its office at The Canadian Venture Building, 82 Richmond St. East, Toronto, Ontario, M5C 1P1.

1.3 SURVEY OBJECTIVES

The objective of this survey is to identify gold-associated sulphide zones and VMS targets in four survey blocks.

2.0 SURVEY AREA

2.1 LOCATION

The survey blocks are located approximately 20 to 50 km east of Dubreuilville, Ontario. They are located within NTS topographic sheets 042-C01, 042-B05, and 042-C08. Figure 1 shows the location of the survey block.

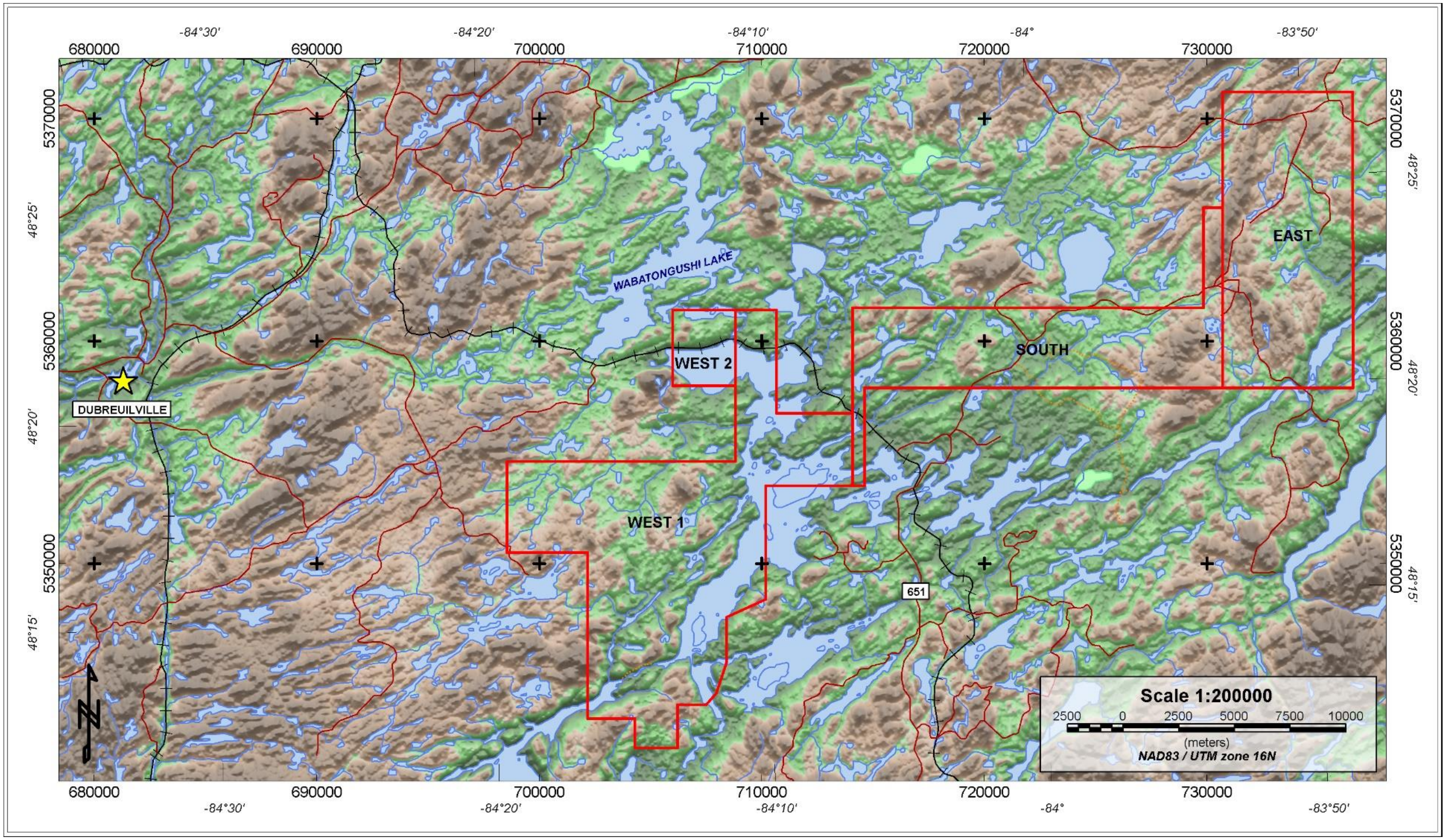

Figure 1 – Survey area showing the four blocks that were flown in red.

2.2 ACCESS

There are logging and dirt roads throughout the area providing access to each survey block

2.3 INFRASTRUCTURE

There is are small towns, hunting lodges, cottages, and logging roads near or within the survey areas.

2.4 CLIMATE

The average daily temperature varies from a high of +24ºC during July to a low of -15ºC during February. During the survey, the weather was variable including high winds, freezing rain, and snow.

2.5 TOPOGRAPHY

The topography is hilly, having a total variation of less than 170 m of elevation variation over the survey area. There are a few lakes within and bordering the survey block area.

2.6 MINERAL AND MINING CLAIMS

The mineral claims are shown in Figure 2. The Client mineral claims are shown in magenta.

2.7 FLIGHT AND TIE LINES

The flight lines are shown in Figure 3 and summarized in Table 1.

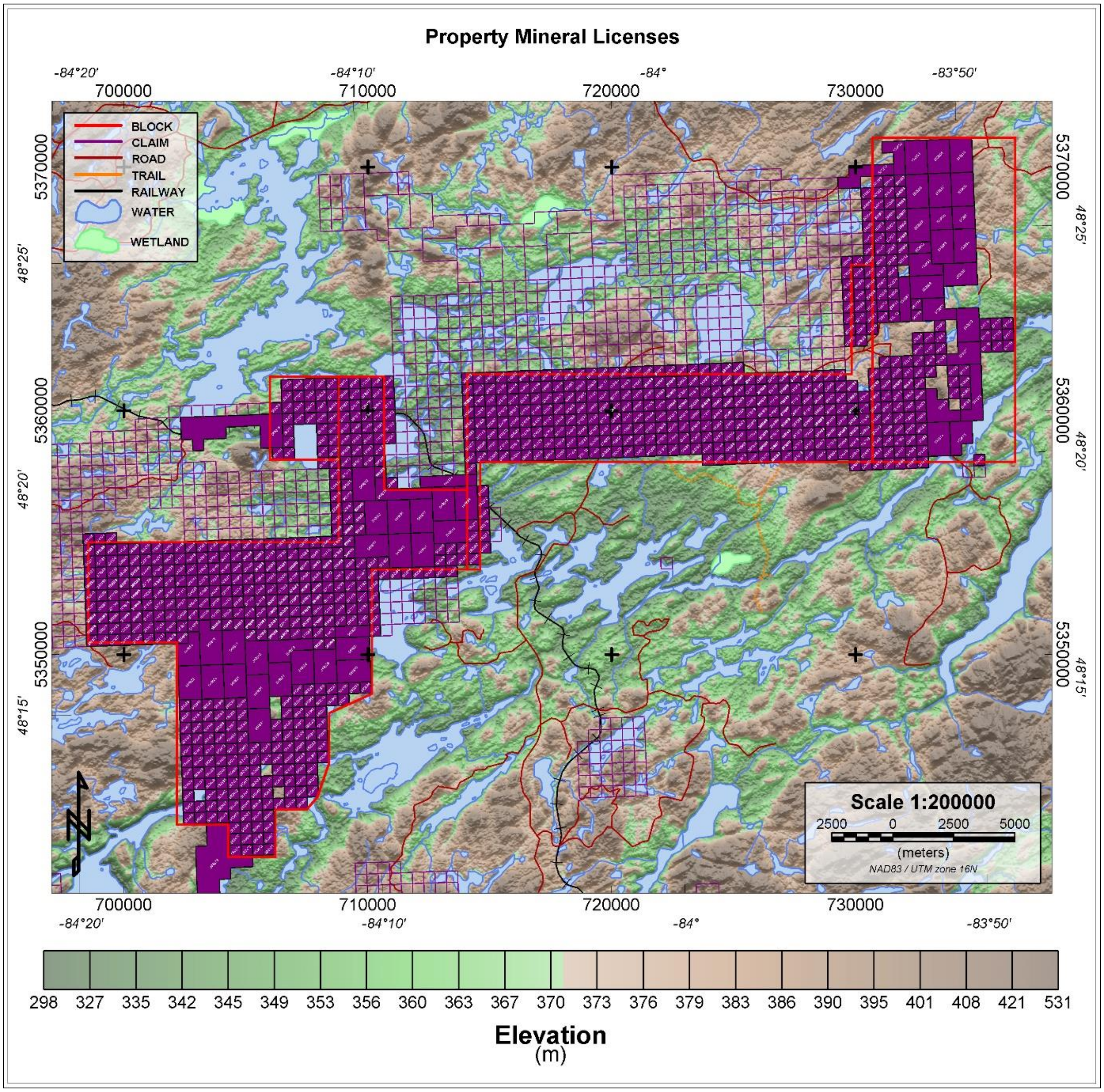

Figure 2 – The mineral claims within the survey blocks.

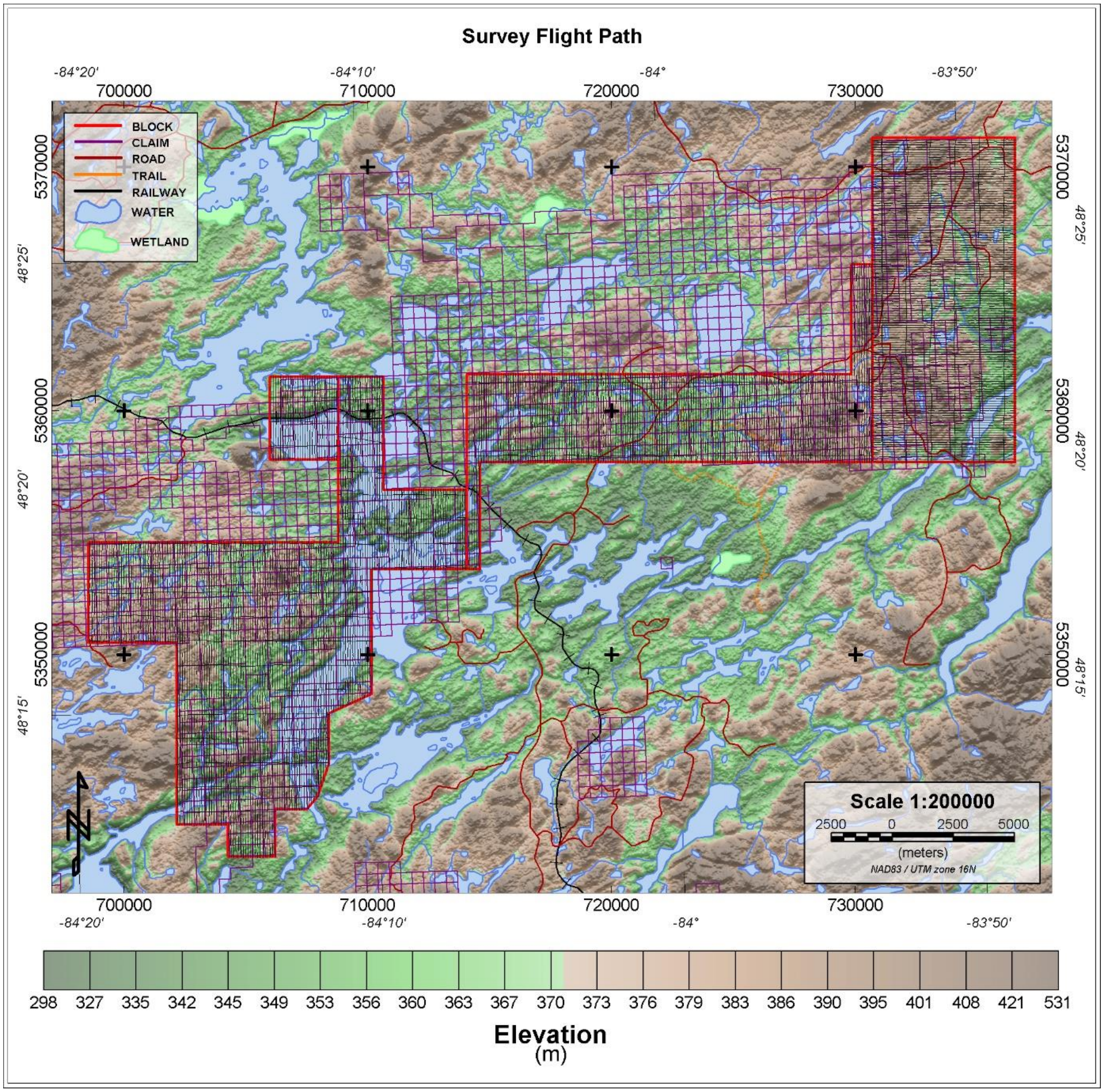

Figure 3 – Flight lines for the survey blocks.

Survey Block	Area (km²)	Line Type	Planned No. of Lines	Line Spacing (m)	Line Orientation	Nominal Survey Height (m)	Total Planned (km)	Total Actual (km)
East	77.81	Survey	133	100	90°/270°	40	778.1	800.1
		Tie	6	1000	0°/180°	40	79.8	81.4
South	66.16	Survey	166	100	0°/180°	40	660.1	684.9
		Tie	12	1000	90°/270°	40	72.2	67.6
West-1	123.42	Survey	155	100	0°/180°	40	1232.2	1301.2
		Tie	19	1000	90°/270°	40	130.4	127.7
West-2	9.59	Survey	38	100	0°/180°	40	95.2	98.3
		Tie	3	1000	90°/270°	40	8.5	8.8
		Total					**3,056.5**	**3,170.0**

Table 1 – Summary of flight and tie line specifications.

2.8 DATUM AND PROJECTION

The survey was flown using the NAD-83 Datum. The Datum used to produce this report as well as the map products, grids and database is NAD-83. The projection is UTM ZONE 16 N. All references to UTM coordinates in this report are based on the NAD-83 Datum.

3.0 SURVEY SYSTEM

The survey system is comprised of an electromagnetic airframe and magnetic sensor housing connected to the helicopter via a tow cable and related and ancillary electronics and sensors inside the helicopter to control navigation, power, and survey height. Combined, this system measures the response from sub-surface conductors containing minerals such as pyrrhotite and pyrite and the magnetic response from features containing minerals such as magnetite. The positions of these responses are measured using a differential GPS antenna and receiver. Flight height is measured by radar altimeter.

3.1 ELECTROMAGNETIC SYSTEM

The electromagnetic system (Figure 4) was developed by Triumph Instruments (Triumph) and is known as AirTEM™, a helicopter time domain electromagnetic (HTEM) system that is designed for mineral exploration, oil & gas exploration and geologic mapping. AirTEM™ is based on the concept of a concentric transmitter and receiver geometry originally developed by Wally Boyko.

The AirTEM™ (TS-150) system features an 8.54 m diameter transmitter weighing approximately 500 Kg and producing up to 150,000 Am² in transmitted power. The system records the full waveform and "X", “Y” and “Z” coil measurements for improved interpretation of complex conductor responses. Measurements of the total magnetic field are also provided.

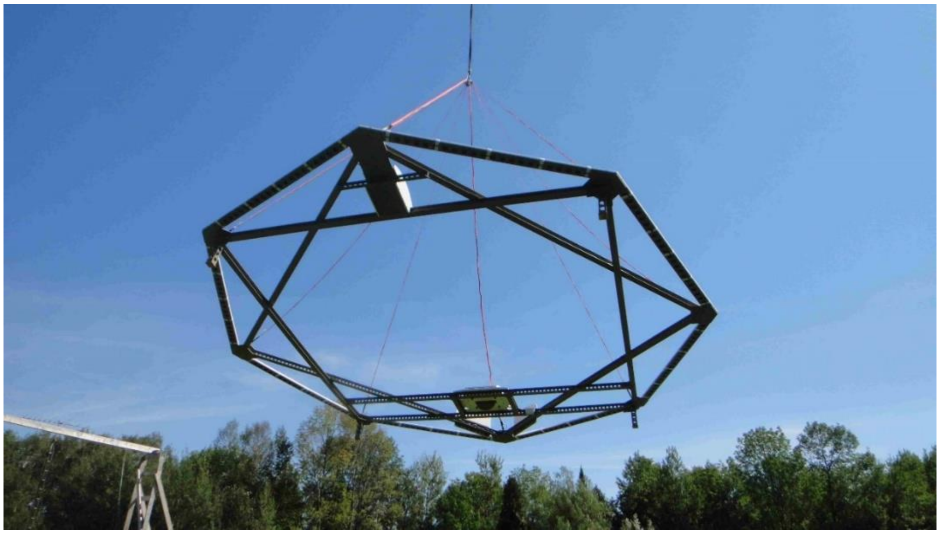

Figure 4 – The Triumph AirTEM^{TM} TS-150 HTEM System.

Features

- Rigid concentric geometry
- Full waveform recording
- Software selectable base frequency
- Software selectable on-time period
- dB/dt off-time and on-time profiles
- Total magnetic field

Advantages

- Excellent early off-time response
- On-time conductance discrimination
- Excellent performance in rugged terrain
- Direct drilling of targets
- Improved nomogram correlation
- Interpretation software readily available

3.2 SYSTEM WAVEFORM

The AirTEM^{TM} system uses a bipolar linear triangular pulse as shown in Figure 5. The on-time pulse is 33% of the half-cycle. The up-going and down-going portions of the pulse are 95% symmetric with the down-going pulse being slightly shorter in time duration.

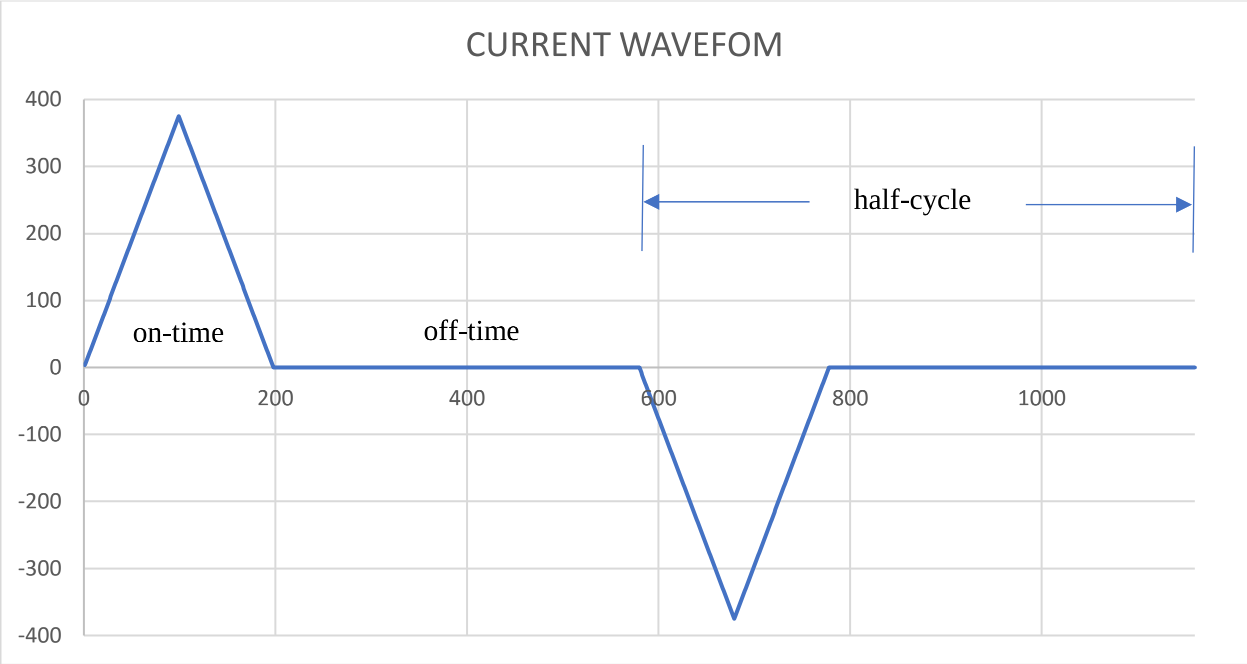

Figure 5 – The transmitter full cycle waveform is bi-polar and triangular with 95% on-time linearity.

3.3 BASE FREQUENCY

This survey was flown using a 90 Hz base frequency. At this frequency the bi-polar waveform produces half-cycles 180 times per second. The total half cycle period is the inverse of 180 Hz or 5,556 µs. For a one third duty cycle the on-time pulse is 1,850 µs in duration and the off-time pulse is 3,704 µs.

The data is stacked to a 10 Hz output sample rate. Each stack is the average of 18 half-cycles, 9 positives and 9 negatives. The negative half-cycles are rectified before being added to the positive cycles. The rectified and stacked half-cycles are stored at the 10 Hz sample rate.

The half-cycle is sampled at 105 kHz or one sample every 9.48 µs producing 580 half-cycle samples, 193 during the transmitter on-time and 387 during the off-time. During the on-time there are 99 up-going samples and 94 down-going samples.

3.4 TIME CHANNELS

The time channels are defined on a logarithmic scale starting at channel 10. Channels 1 through 9 are linearly spaced, have a 5 µs width and start 10 µs after the end of the on-time pulse. For a 90 Hz base frequency there are 41 off-time channels. The time channels used are listed in Table 2.

Channel	Start time (ms)	Channel	Start time (ms)
1	0.0100	26	0.4199
2	0.0150	27	0.4810
3	0.0200	28	0.5512
4	0.0250	29	0.6320
5	0.0300	30	0.7249
6	0.0350	31	0.8317
7	0.0400	32	0.9545
8	0.0450	33	1.0957
9	0.0500	34	1.2581
10	0.0557	35	1.4448
11	0.0622	36	1.6595
12	0.0698	37	1.9063
13	0.0784	38	2.1901
14	0.0884	39	2.5164
15	0.0998	40	2.8916
16	0.1130	41	3.3230
17	0.1281	42	3.8190
18	0.1455	43	4.3893
19	0.1655	44	5.0451
20	0.1885	45	5.7992
21	0.2150	46	6.6662
22	0.2454	47	7.6631
23	0.2803	48	8.8093
24	0.3205	49	10.1273
25	0.3667	50	11.6427

Table 2 – Time channels for the TS-150.

3.5 MAGNETIC SYSTEM

The airborne magnetometer system consists of the housing, the sensor and control module and Larmour frequency counter. The counter output rate is 10 Hz in digital RS 232 format. Power is provided to the sensor electronics via a 28 VDC power cable on the tow cable which is terminated to a 5-pin connector at the magnetometer housing. This cable also contains conductors that carry the RS 232 signal.

3.6 MAGNETOMETER SENSOR

The magnetometer sensor is a model CS-3 made by Scintrex Limited. It is an optical split-beam cesium magnetometer and consists of a sensor head with a 3-m cable connected to a sensor driver. The output of the sensor driver is a larmour frequency which is linearly proportional to the earth's magnetic field. The CS-3 is shown in Figure 6 and the sensor specifications are given in Table 3.

Figure 6 – Scintrex CS-3 magnetometer sensor, cable and electronics.

3.7 LARMOUR COUNTER

The larmour frequency is input into a frequency counter made by Triumph Instruments. The counter can convert the magnetic field to a theoretical accuracy of 0.2 pT. The output of the frequency counter is a digital value of the magnetic field with +/- 0.001 nT resolution. This value is transmitted to the EM console at a 10 Hz output rate.

The larmour counter is not synchronized to the EM transmitter but is synchronized instead to the EM data system. This allows the frequency counter to average down the magnetic field caused by the on-time pulse from the EM transmitter. The noise resulting from lack of synchronization to the EM transmitter is removed using a high-cut frequency filter during processing which also removes the effects of drop-outs when the magnetometer sensor loses lock with the magnetic field (common during turn-arounds).

3.8 SENSOR HOUSING

The magnetometer sensor housing is made from a thin-wall fiberglass tube (see Figure 7). The manufacturer is AeroComp of London, Ontario. Within the housing a two-axis gimbal holds the sensor and can be rotated in both the horizontal and vertical plane. The sensor was set to the point 45^{o} degrees forward with a 25^{o} azimuth for this survey. The housing contains the sensor driver electronics and the larmour frequency counter.

Operating Principal	Self-oscillation split-beam Cesium Vapor (non-radioactive Cs-133)
Operating Range	15,000 to 105,000 nT
Gradient Tolerance	40,000 nT/meter
Operating Zones	10° to 85° and 95° to 170°
Hemisphere Switching	a) Automatic b) Control voltage c) Manual
Sensitivity	0.0006 nT √Hz rms
Noise Envelope	Typically, 0.002 nT P-P, 0.1 to 1 Hz bandwidth
Heading Error	+/- 0.25 nT (inside the optical axis to the field direction angle range 15° to 75° and 105° to 165°)
Absolute Accuracy	<2.5 nT throughout range
Output	a) Continuous Larmor frequency proportional to the magnetic field (3.49857 Hz/nT) sine wave signal amplitude modulated on the power supply voltage b) Square wave signal at the I/O connector, TTL/CMOS compatible
Information Bandwidth	Only limited by the magnetometer processor used
Sensor Head	Diameter: 63 mm (2.5”) Length: 160 mm (6.3”) Weight: 1.15 kg (2.6 lb)
Sensor Electronics	Diameter: 63 mm (2.5”) Length: 350 mm (13.8”) Weight: 1.5 kg (3.3 lb)
Cable, Sensor to Sensor Electronics	3 m (9’ 8”), lengths up to 5 m (16’ 4”) available
Operating Temperature	-40°C to +50°C
Humidity	Up to 100%, splash proof
Supply Power	24 to 35 Volts DC
Supply Current	Approx. 1.5 A at start up, decreasing to 0.5 A at 20°C
Power Up Time	Less than 15 minutes at -30°C

Table 3 – Scintrex CS-3 specifications.

Figure 7 – Airborne magnetometer housing with tow cable.

3.9 BASE STATION MAGNETOMETER

A GSM-19 base station magnetometer (manufactured by Gem Systems) was used to record variations in the earth's magnetic field and referenced into the master database using a GPS UTC time stamp. This system is based on the Overhauser principle and records the total magnetic field to within +/- 0.02 nT at a one (1) second time interval.

The base station unit was erected in a geomagnetically quiet location near Dubreuilville, ON.

Figure 8 – Base station magnetometer used for diurnal corrections.

3.3 NAVIGATION

Navigation was provided by the AgNav Incorporated (AgNav-2 version) GPS navigation system (Figure 9 - left) for real-time locating while surveying. The AgNav unit was connected to a Tee-Jet GPS receiver (Figure 9 – right).

Also used was a Garmin 19x antenna and receiver located on the HTEM airframe. The Garmin 19x, which is capable of sub five-meter accuracy, was sampled at 10 Hz.

Figure 9 – AgNav main console (left) and Tee-Jet GPS receiver (right).

3.4 RADAR ALTIMETER

The radar altimeter transmitter and receiver antenna were fixed to the rear skids of the helicopter (one antenna on each skid) approximately 36" apart. The coaxial cables were fed through the floor of the helicopter and routed along the floor. Both coaxial cables connected to the controller which was located near the TDEM-2400 control unit. On the output side of the controller (Figure 10 - left) a proprietary 16-bit A/D convertor was connected proving digital input to the TDEM-2400 via RS 232 format. The altimeter signal was also fed into a digital read-out unit (Figure 10 - right) mounted on the dashboard of the helicopter in clear vision of the pilot to provide height above ground navigation.

Figure 10 – Freeflight radar altimeter controller and digital readout.

3.5 HELICOPTER

The helicopter used (Figure 11) was an AS 350 D2 with registration C-FJPI, owned and operated by Expedition Helicopters and based in Cochrane, Ontario.

Figure 11 – The survey used an AS 350 D2 as shown above.

3.6 PERSONNEL

The following personnel were involved in the survey.

Individual	Position	Description
Mark Cusack	Pilot	Helicopter pilot
Dan LeBlanc	Operator	Operated and maintained the equipment
Steve Balch	Field Processing	On-site data processing
Steve Balch	Final Processing	Line-leveling, drift correction, diurnal corrections, tie-line leveling
Mike Cunningham	Reporting	Report write-up
Steve Balch	Supervision	Liaison with Client. Responsible for the crew
Chris Balch	Mapping	Plotting maps, printing report, folding and binding
Richard Murphy	Client	CEO

Table 4 – Summary of Personnel.

4.0 DATA ACQUISITION

4.1 HARDWARE

Data was collected through the main console (the TDS-2400, see Figure 12) which contained both the acquisition system and dc-dc power control module (booster circuit) for the transmitter coil. The TDS-2400 has a hardware controller that sets the timing for the four (4) 24-bit A/D converters that sample at 9.48 µs. The controller also generates and transmits the timing control signals to the transmitter driver located on the airframe.

The main controller also performs synchronization between the transmitter and receiver and all ancillary information (GPS, MAG, EM, RAD ALT). The ancillary information is digitized and stored at a rate of 10 Hz. The resulting data string is transmitted to a laptop computer and stored on an internal hard drive.

Figure 12 – Triumph TDS-2400 EM console and acquisition system.

4.2 SOFTWARE

A rugged laptop computer running the Windows 10 operating system controls the incoming data stream from the TDS-2400. The software on the laptop (AirDAS) is capable of real-time acquisition with no data loss from 25 Hz to 300 Hz for a duty cycle that can vary from 10% to 50% (nominally set at 30-35%).

During the survey the Operator can monitor the incoming differential GPS data, radar altimeter, magnetometer and all EM profiles.

After each flight data is copied from the laptop internal hard drive onto a memory stick. While there is no limit on the maximum file size during acquisition, the processing software can only process up to five (5) continuous hours of recorded data. For longer flights the data can be broken into two files.

4.3 CALENDAR

Data was acquired over a 15-day (Table 5) period. Mobilization occurred on March 24th from Rockwood, Ontario and arrived at Dubreuilville, Ontario the same day. Assembly of the system took place at on March 25th. Production commenced on March 26th and was completed on April 6th. The system was de-installed on April 6th and demobilized to Rockwood, Ontario occurred on April 7th.

Sunday	Monday	Tuesday	Wednesday	Thursday	Friday	Saturday
Mar. 22	Mar. 23	Mar. 24	Mar. 25	Mar. 26	Mar. 27	Mar. 28
		Mob	Install	FLT-01, FLT-02	FLT-03, FLT-04	FLT-05, FLT-06
Mar. 29	Mar. 30	Mar. 31	Apr. 01	Apr. 02	Apr. 03	Apr. 04
Standby	FLT-07	FLT-08	FLT-09, FLT-10	FLT-11, FLT-12	FLT-13, FLT-14	Standby
Apr. 05	Apr. 06	Apr. 07	Apr. 08	Apr. 09	Apr. 10	Apr. 11
FLT-15, FLT-16	FLT-17, De-install	Demob				

Table 5 – Time schedule of the survey.

5.0 DATA PROCESSING

Preliminary data processing is performed using BECI proprietary methods. This includes compensation, filtering and line leveling of the HTEM data. This also includes calculation of the vertical magnetic gradient, analytic signal, digital terrain model, bird height, and merging of the base station magnetic data (sampled at 1.0 sec) with the survey data (sampled at 0.1 sec).

5.1 NAVIGATION

The helicopter pilot uses “ideal” flight lines as guidance during surveying as displayed on the real-time AgNav system with the aid of a helicopter mounted GPS. A separate GPS mounted to the bird is used to record actual position. The sample rate of the GPS is 10 Hz, the same as the EM, MAG and ancillary data collected in flight.

The GPS unit outputs both latitude, longitude and easting, northing values, all in the NAD-83 Datum, using a UTM Projection. The positional data is not filtered but occasional bad data points are interpolated using a linear algorithm.

5.2 TERRAIN CLEARANCE

The radar altimeter is located under the base of the helicopter. The helicopter mounted radar altimeter is used to maintain terrain clearance by the pilot. A digital indicator is mounted on the dashboard of the helicopter. This installation is approved by a licensed helicopter engineer provided by the helicopter operator.

5.3 EM DATA PROCESSING

The EM data is processed using BECI proprietary software designed to compensate, filter and level both the off-time and on-time data.

The first step in processing is to determine the transmitter shut-off time and align the time gates to this position. The length of time that the transmitter is on is known as the on-time. The time gates are logarithmically spaced in the off-time and linearly spaced in the on-time.

The second processing step is the calculation of the system background transient. This is done at a suitable flight height, nominally 1,000 feet or higher. During this time EM data is collected for a period of 50 seconds and averaged into a single background transient. This is subtracted from the transients recorded online.

The third step is to assign the flight line numbers to each data point so that the flight can be separated into flight lines within Geosoft.

Line-leveling and drift-correction are achieved on a flight by flight basis using the background transients, recorded at the start and end of each flight.

Filtering the data involves a two-step process. Spikes are removed using an algorithm based on the Naudy non-linear filtering algorithm. This is followed by a 61-point Hanning filter that has the effect of smoothing the profiles over an equivalent distance of approximating twice the nominal flight height.

Micro-leveling of the late time channels is also performed before the data file is written to disk. Conductor picks and Tau time constants are determined at this point as well.

B-field processing of the time channels uses a fully integrated on-time in addition to the integrated off-time (i.e. full waveform). The early off-time channels are evaluated for possible primary field leakage (this involves a compensation filter based on linearly derived correlation between the late on-time and early off-time samples). The exact methodology is considered proprietary.

5.4 MAGNETIC DATA PROCESSING

The magnetic data (i.e. MAG from the airborne sensor and BMAG from the ground sensor) is collected without a lag time (i.e. synchronous with the HTEM data and UTC time), therefore a lag time correction is not applied. In areas where the MAG sensor has become unlocked (e.g. most often during turn-arounds), the total magnetic field values are replaced with a dummy value ("*") and the data is later interpolated in Geosoft.

The raw ASCII survey data files and BMAG ASCII data files are imported into BECI software and merged using UTC time, common to both files. A quality control check of the BMAG data is made on a day to day basis.

Diurnal magnetic corrections are applied to the MAG data using the BMAG data. The base station data (i.e. BMAG) is linearly interpolated from a 1.0 sec sample rate to 0.1 sec to correspond to the flight data after the BMAG has been filtered with a 60 second filter.

Once the diurnal field is subtracted from the MAG data, a heading correction is applied and the resulting total magnetic intensity (TMI) is micro-leveled.

6.0 RESULTS

The total magnetic intensity (TMI) is shown in Figure 13, reduced to pole is Figure 14, 1st vertical derivative is Figure 15, analytic signal is Figure 16, and the tilt derivative is Figure 17.

The anomalous EM response is shown in Figure 18 (early off-time), Figure 19 (mid off-time), and Figure 20 (late off-time).

Figure 21 shows the digital terrain model for the survey area.

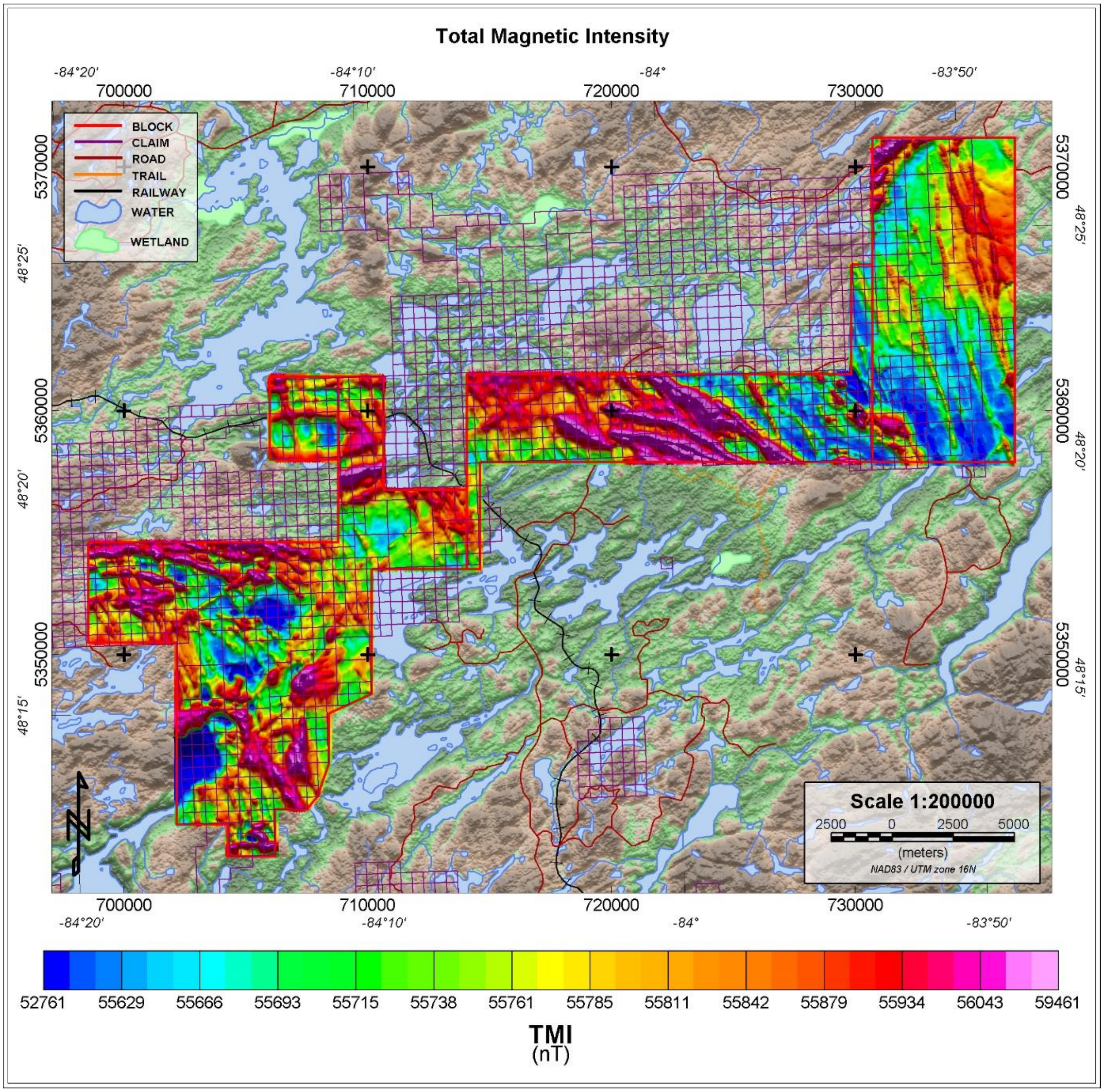

Figure 13 – Shaded image of the Total Magnetic Intensity (TMI) over the blocks.

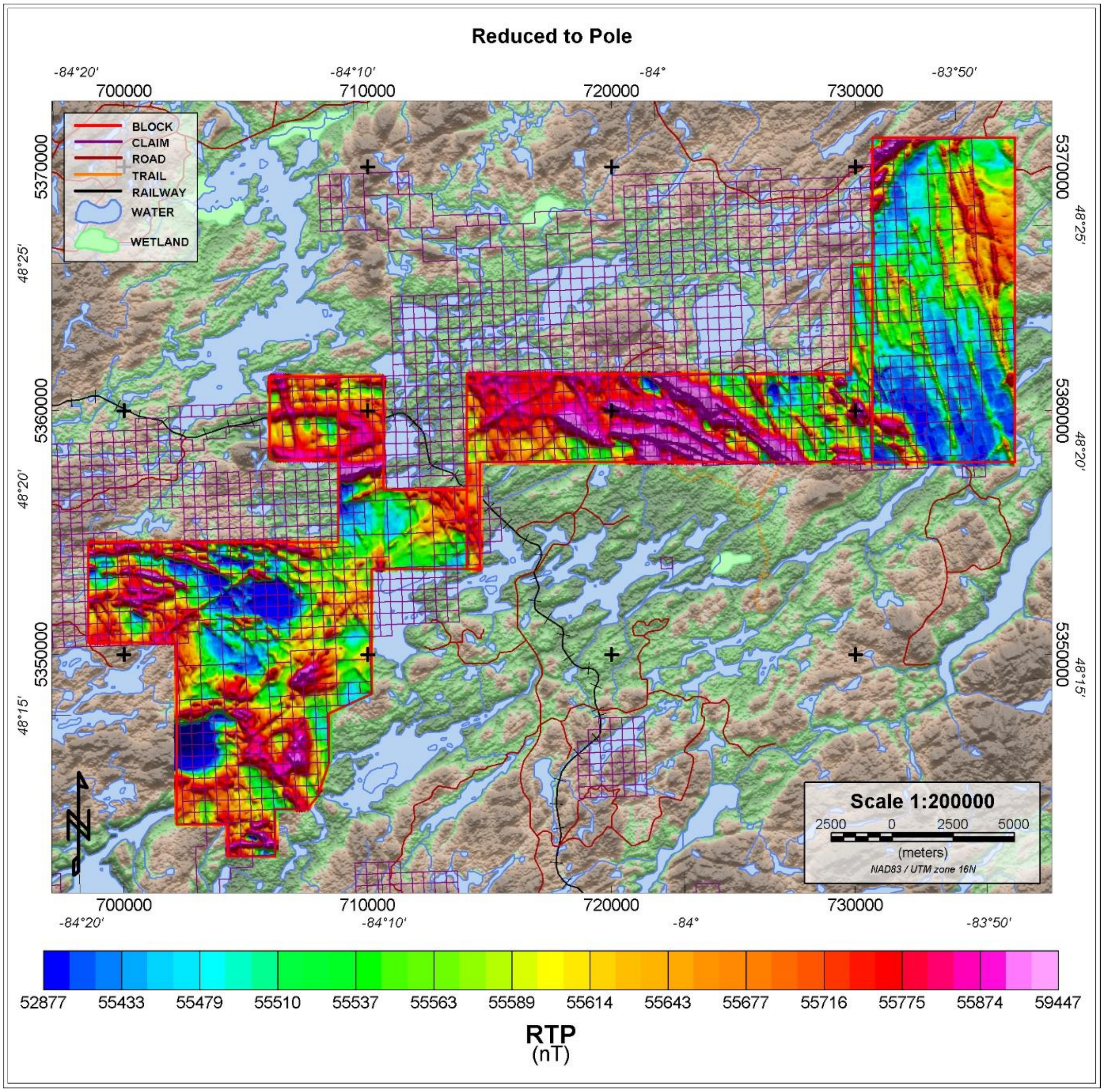

Figure 14 – Shaded image of Reduced to Pole (RTP) TMI over the blocks.

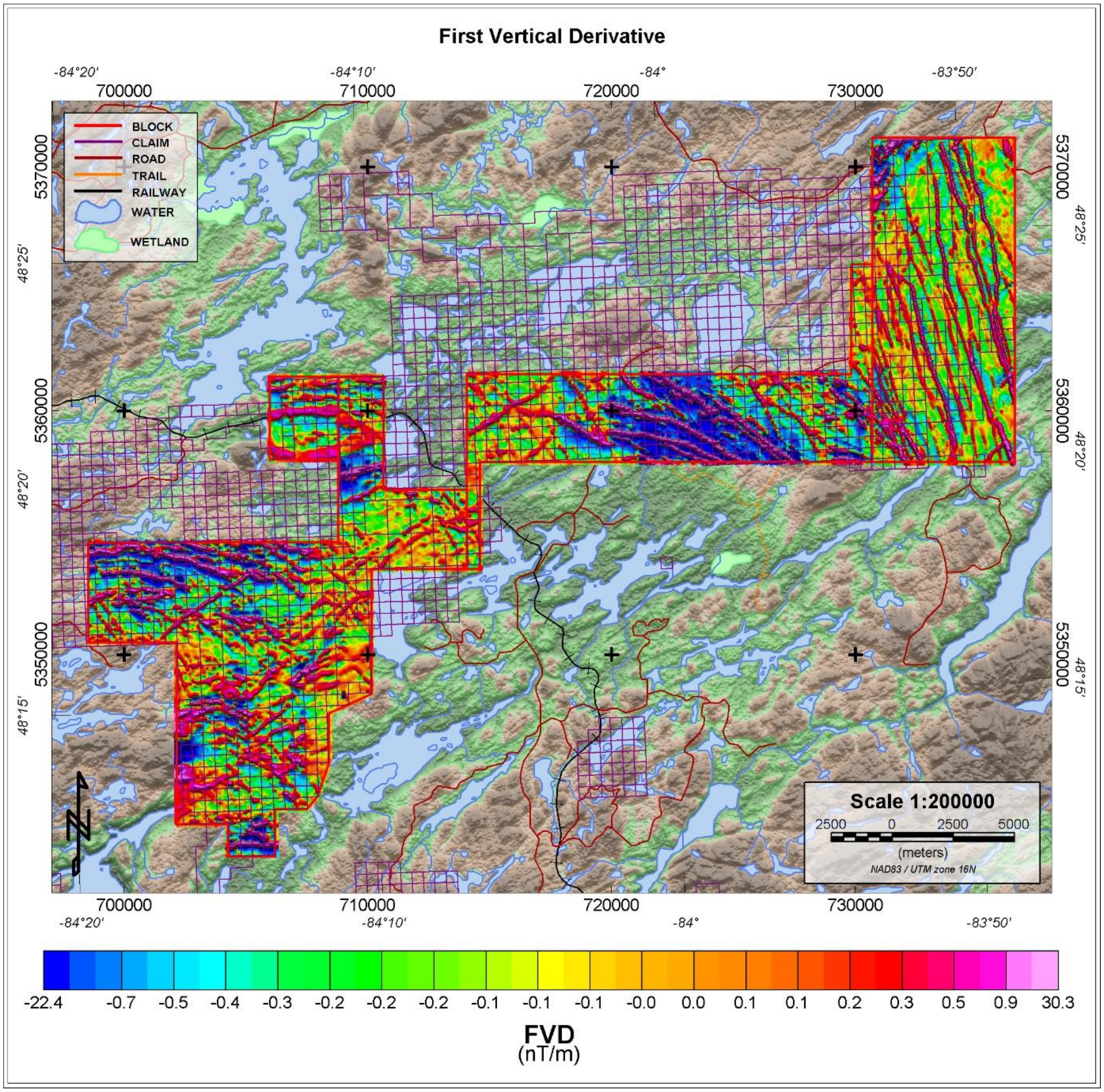

Figure 15 – Shaded image of the Frist Vertical Derivative (FVD) over the blocks.

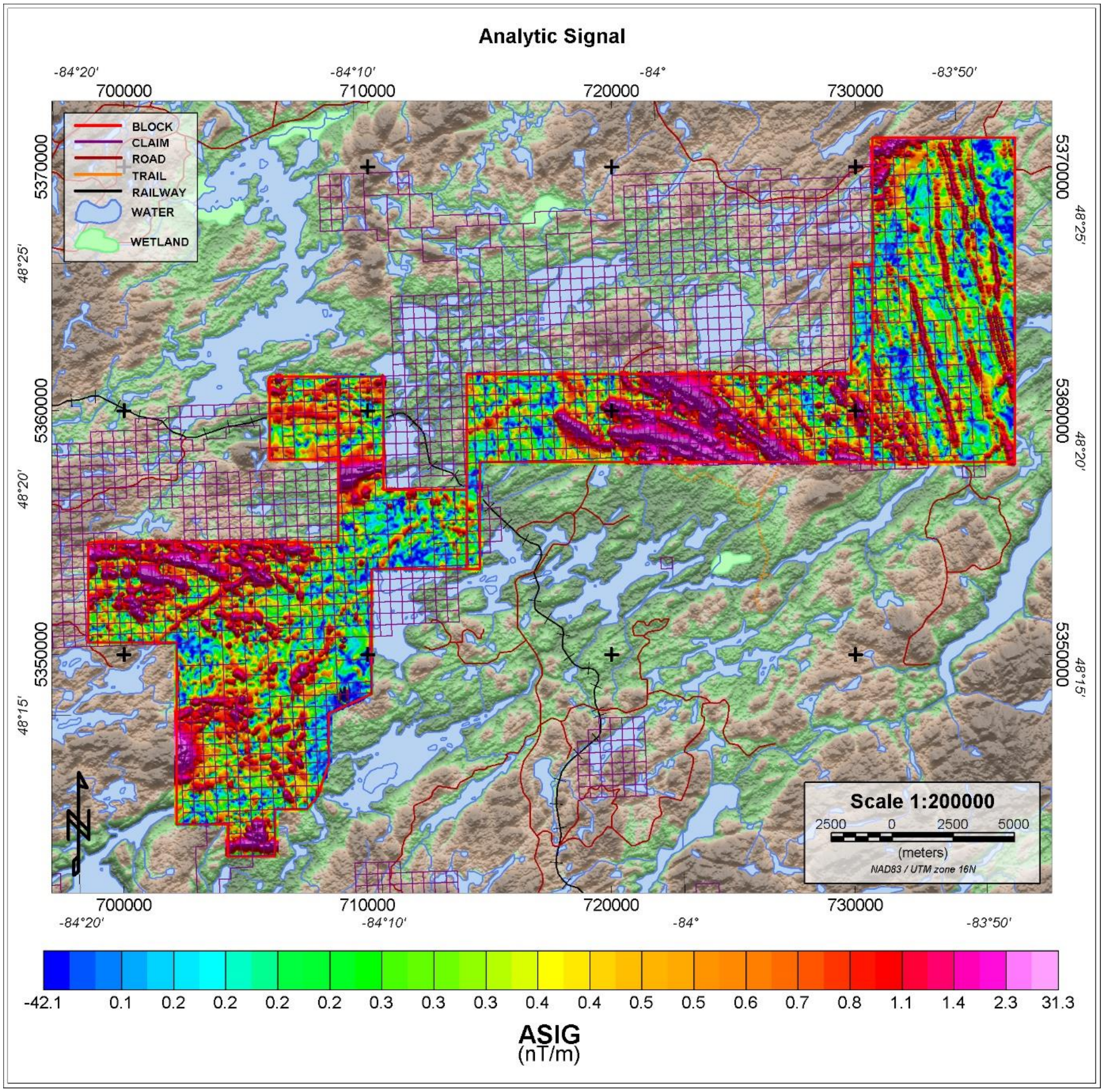

Figure 16 – Shaded image of the Analytic Signal (ASIG) over the blocks.

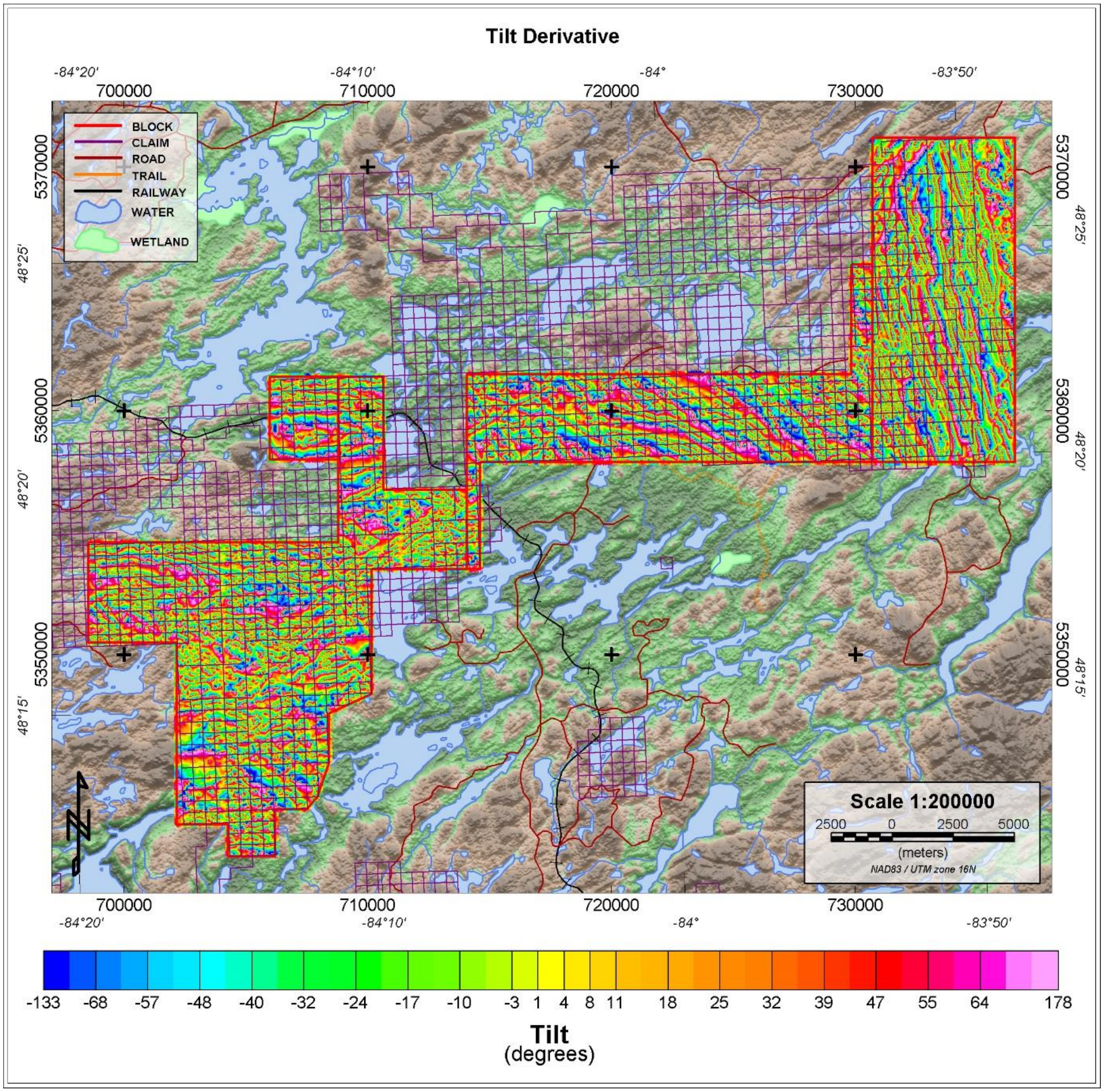

Figure 17 – Shaded image of the Tilt Derivative over the blocks.

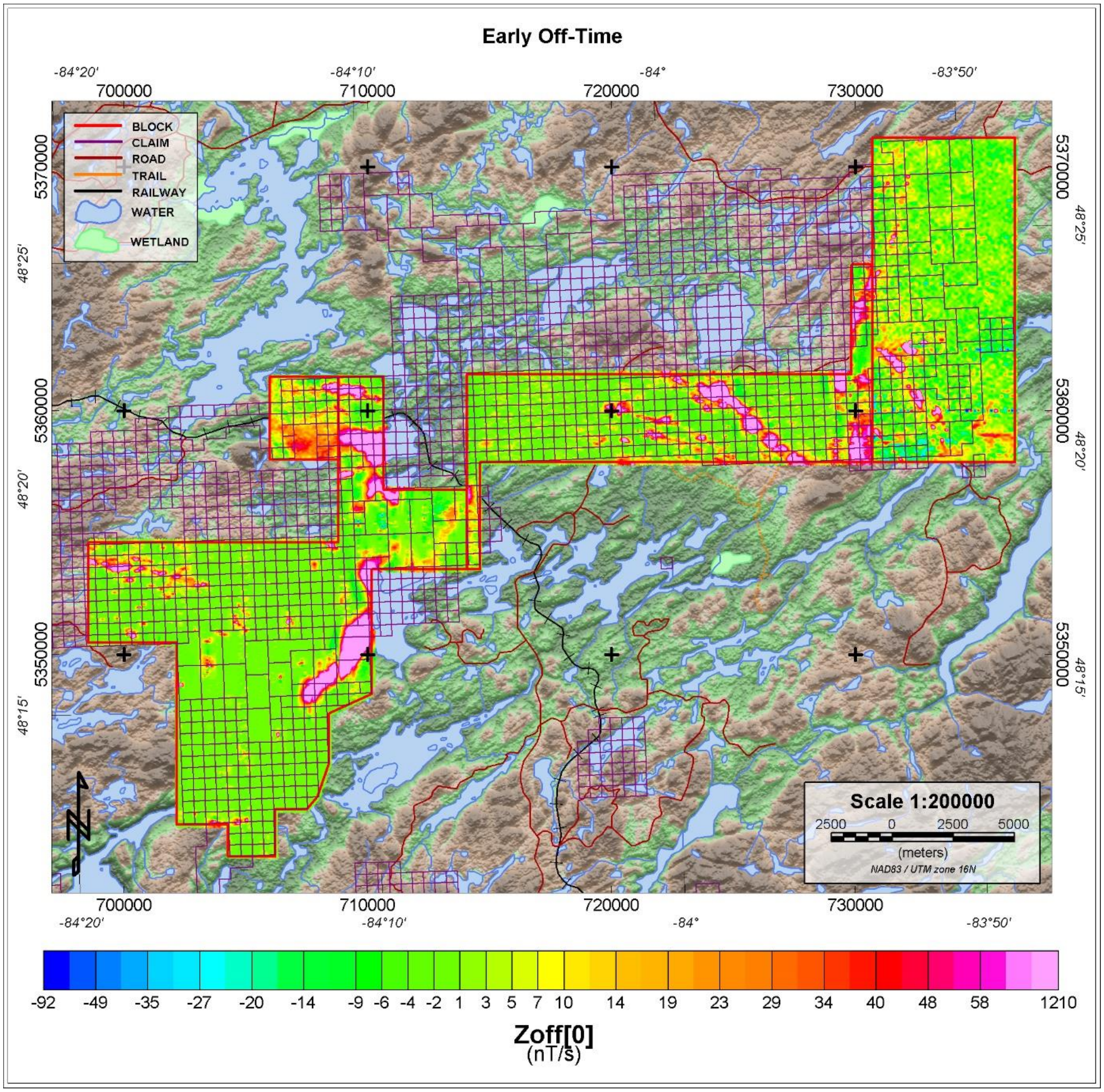

Figure 18 – Image of the Early Off-Time (Zoff[0]) over the blocks.

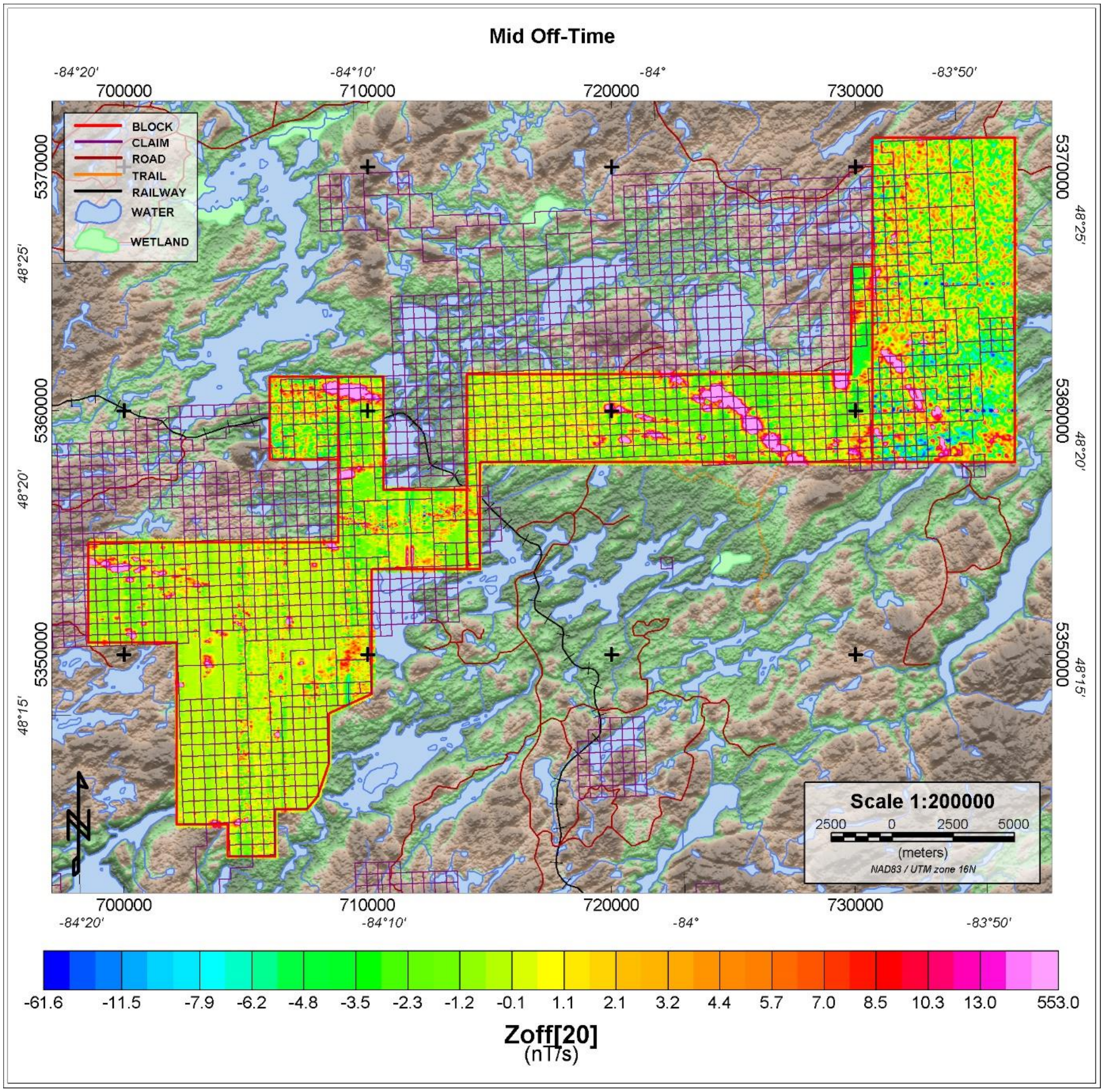

Figure 19 – Image of the Mid Off-Time (Zoff[20]) over the blocks.

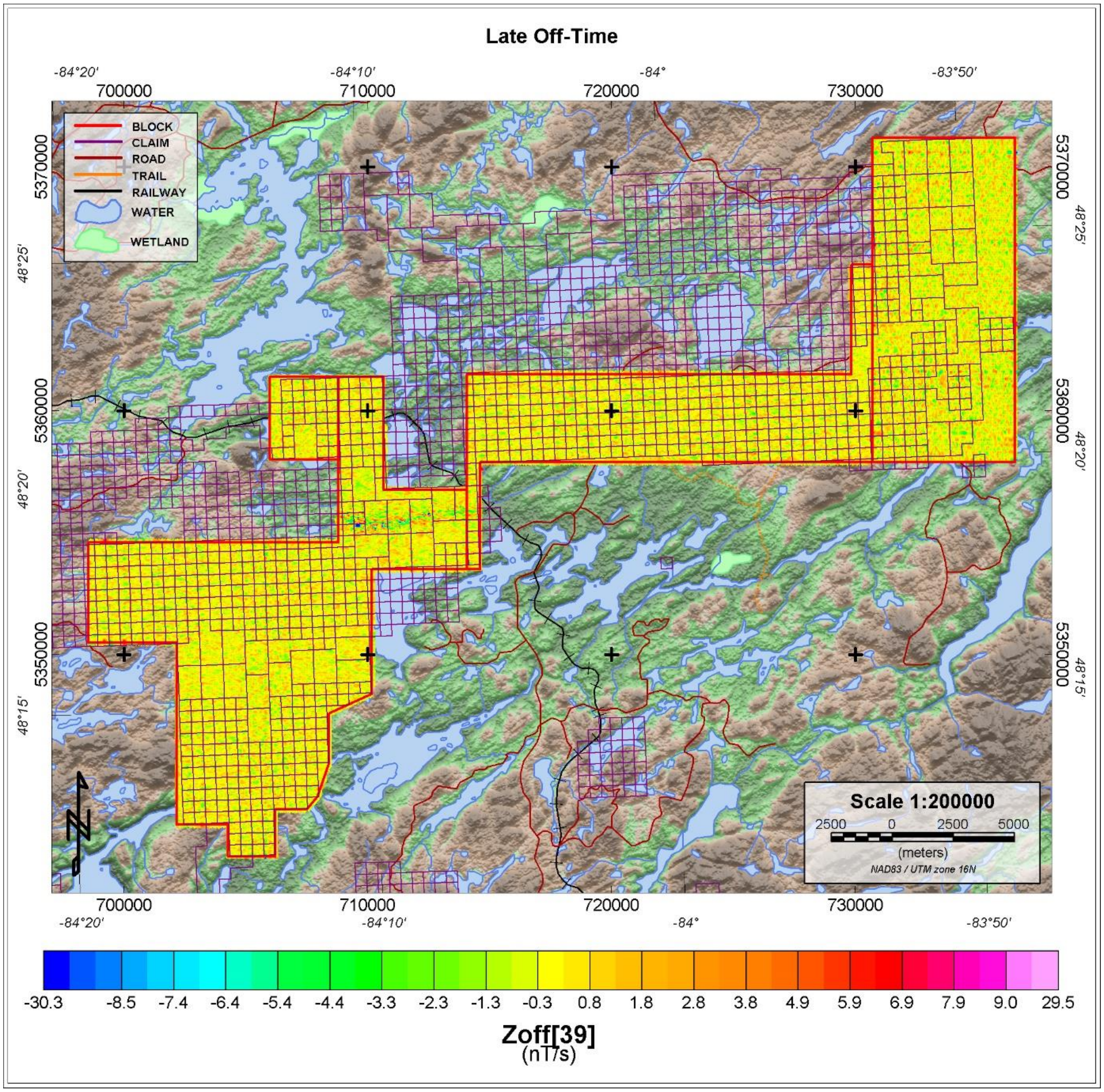

Figure 20 – Image of the Late Off-Time (Zoff[39]) over the blocks.

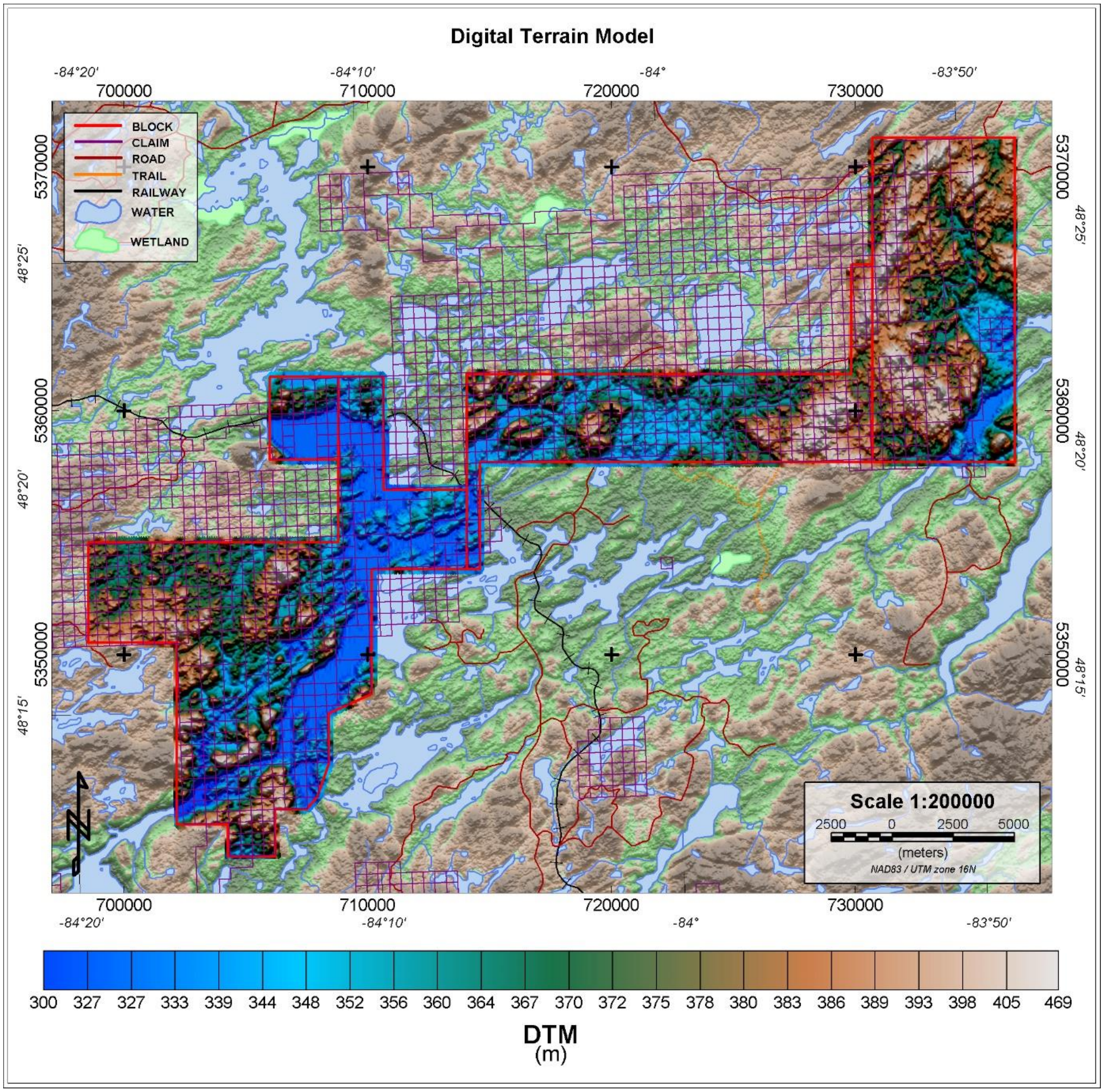

Figure 21 – Shaded image of the Digital Terrain Model (DTM) over the blocks.

7.0 INTERPRETATION

7.1 OVERVIEW

The Goudreau Project, has been covered by several airborne geophysical surveys, some overlapping, but not totally contiguous (leaving some areas uncovered).

The survey with the largest lateral coverage was completed in 1988 using the Dighem HEM system for a total of 20,224 l-km and a 200 m line spacing. The survey is considered to have a lateral positional error averaging 20-40 m. Both frequency domain EM and magnetics were acquired. Figure 22 shows the total airborne coverage as individual red polygons within a location map highlighting Dubreiville and Wawa.

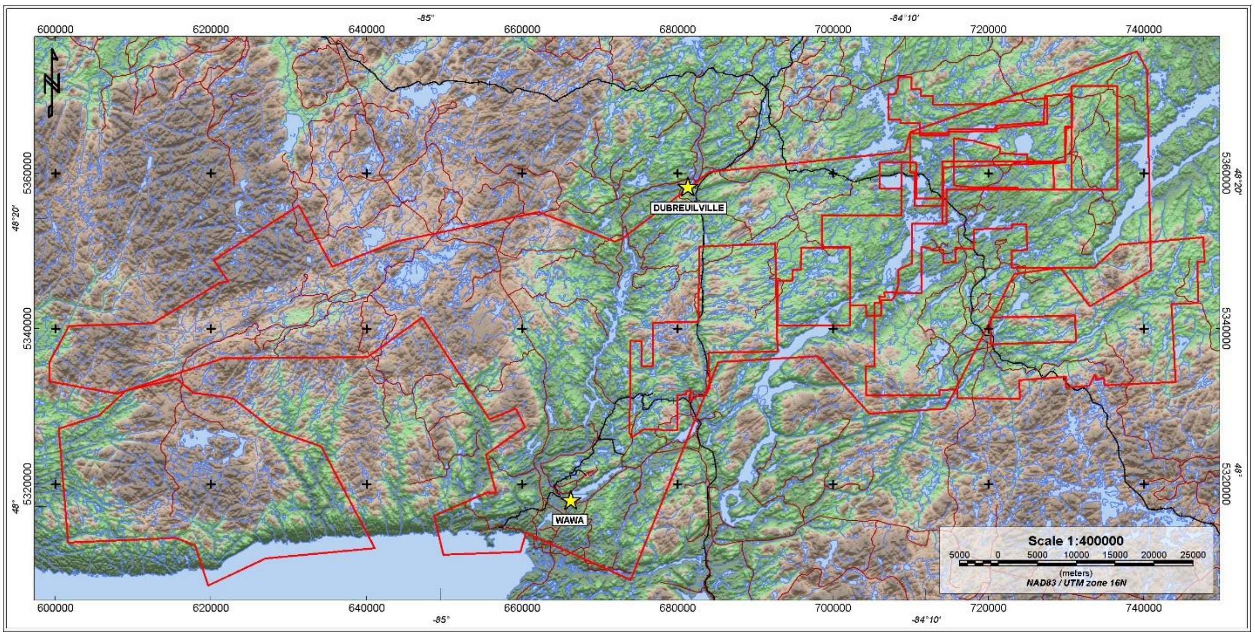

Figure 22 - Location map of Goudreau Project showing the overall airborne survey coverage.

In 2006 an AeroTEM time domain EM and magnetic survey was flown for Ridgeline Resources over the northern portion of the property totaling 801 l-km based on 100 m spaced lines, oriented north-south. In 2011 the area flown in 2006 was re-flown by CMG Airborne using a high-resolution magnetic gradiometer. A total of 846 l-km was acquired along north-south lines spaced 100 apart.

In 2011 the area was flown using VTEM and consisted of four blocks (Magpie1, Magpie2, Magpie3 and Magpie4) in various locations. Magpie1 totaled 1,686 l-km and was located contiguous to, and south of, the AeroTEM block with north-south lines spaced 75 m apart. The Magpie2 block, totaling 3,528.9 l-km, is located 43km southwest of the AeroTEM block and was flown using a north-south flight line orientation and 75 m spacing. The Magpie3a block was located 35 km southwest of the original AeroTEM block and consisted of north-south flight lines spaced 75 m and totaling 1,183.5 km. The Magpie3b block was located 28 km south of the AeroTEM block and was flown with a line spacing of 75 m in both the north-south and east-west directions, totaling 922.7 l-km. The Magpie4 block was flown using a 75 m flight line spacing oriented north-south and totaling 951.9 km. Magpie4 was a superset of Magpie3b with the former completely overlapping (and expanding) the latter.

7.15 REGIONAL GEOLOGY

The following description of regional geology is derived from Heather and Arias (1992)*. The Goudreau property is located within the Goudreau-Lochalsh area of the Wawa Subprovince of the Superior Province in the Canadian Shield. The Wawa subprovince is west of the Kapuskasing Structural Zone and south of the Quetico subprovinces. The property is within Archean supracrustal rocks, a greenstone belt known as Michipocoten, and is interpreted as a monoclinical sequence that has been thickened by regional folding (two phases of folding) which consists of felsic to intermediate, pyroclastic metavolcanics and topped with pyrite-bearing iron formation. To its the north are pillowed, massive, and schistose mafic to intermediate metavolcanic rocks. Felsic intrusions range in composition from nepheline syenite to tonalite/trondhjemite over the Goudreau-Lochalsh area. The supracrustal rocks have a metamorphic grade of greenschist, except to the north where grades range from amphibolite to external tonalite-granodiorite granitoid rocks. Northwest- and northeast-striking diabase dikes cross-cut all other rock units.

Two subparallel, regionally extensive, zones of deformation are referred to as the Goudreau Lake Deformation Zone (GLDZ) and the Cradle Lakes Deformation Zone (CLDZ). Both zones have been defined using deformation intensity of the supracrustal rocks, deformation style, and distribution and density of discrete high-strain zones. Most gold occurrences are located within the GLDZ, which is 30 km long, east-northeast to east striking zone subparallel to lithological and foliation trends. The GLDZ can be subdivided into four structural domains based on deformation, lineation, and orientation and sense of shear displacement. To the north is the Loch Lomond Deformation Zone and northeast are the Missinaibi, Baltimore, and Easy Lake Deformation Zones. South of the GLDZ is the CLDZ, which is at least 5-10 km in length and 1-2 km in width.

Gold mineralization has been associated to high-strain zone hosted quartz veins that can be hosted by all rock types excluding diabase dikes. Furthermore, there is a spatial association of gold mineralization with felsic porphyry dikes and stocks. Deformation of gold zones is confined to discrete high-strain zones. Intense alteration has been observed of mafic rocks to an assemblage of biotite, Fe-carbonate, pyrite, pyrrhotite, quartz, potassium feldspar (minor), chlorite, and/or calcite. Alteration of felsic rocks to assemblages of quartz, sericite, pyrite, Fe-carbonate, albite, hematite, pyrite, chlorite (replacing sericite) and/or pyrrhotite.

***REFERENCE**

Heather, K. B. and Arias, Z. 1992. *Geological and structural setting of gold mineralization in the Goudreau-Lochalsh area, Wawa gold camp*. Ontario Geological Survey, Open File Report 5832, 159p.

7.2 STYLES OF MINERALIZATION

The mineralization at Goudreau is primarily shear-zone hosted gold. Mineralization can occur within quartz veins and veinlets or within sulphide zones that have been sheared and altered (silicified and carbonatized).

Such targets typically do not have magnetic or electromagnetic responses directly. In the presence of magnetite-rich iron formation, however, the mineralization can be magnetic and conductive.

Also present is volcanogenic style massive sulphide (VMS), rich mainly in zinc (sphalerite) but also with minor copper (chalcopyrite) and lead (galena). Such deposits are conductive and respond well to electromagnetic methods but in the case of shear zones where the geology is highly faulted conductors can be multiple in number and small in surface area making them difficult to detect unless close to surface using high dipole moment systems with a small flight line spacing (e.g. 50 m).

The gold mineralization is associated with secondary shear zones and/or lithologic contacts that transect the main shears at 60° and 120° angles. Where the dominant strike direction is east-west, mineralized structures can be expected to strike approximately at 60°/120° although local folding can alter the strike direction somewhat.

Airborne geophysical surveys will map the general geology and can highlight shear zones and faults based on discontinuities in the magnetic field data. Formational conductors, due mainly to inter-connected sulphide such as pyrrhotite and pyrite, are well defined by electromagnetic methods. Such features can act as marker horizons especially where mineralized structures intersect (disrupting the continuity of) the formational trends.

7.2.1 Stover Prospect

Mineralization at Stover is described as moderate to low-grade gold found over relatively thick intersections (e.g. 42.5 m of 0.4 g/t Au in SL-88-01). The host rocks are silicified quartz-sericite schist. The main exploration tool has been induced polarization with the mineralization exhibiting elevated chargeability and high resistivity. The central location of Stover is 725,900 mE and 5,359,900 mN. Drilling has outlined an area of mineralization along a 400 m strike length trending 120º.

7.2.2 Rockstar Prospect

Mineralization at Rockstar is typically higher-grade zones over narrow intervals (e.g. 5.0 g/t Au over 4.6 m in MTU-20-16 including 11.1 g/t Au over 1.2 m). Mineralization occurs within a quartz vein system that is sheared and altered by carbonatization and silicification. Such alteration usually destroys any interconnection of sulphide minerals suggesting high resistivity. The central location of Rockstar is 703,490 mE and 5,353,440 mN. Based on drilling, the gold mineralization at Rockstar appears to show a steep plunge to the west.

7.2.3 Tracenelli Prospect

Mineralization at Tracenelli is described as moderate to high-grade gold (1-10 g/t Au) in quartz veins of varying width (1-7 m), having discrete strike lengths to 30 m and being located very close to surface (20-30 m below ground). Mineralization occurs within structures that are parallel to regional structural trend (150º) but also at up to 60º angles (typically around 110º). The central location is 703,450 mE and 5,349,125 mN. Based on descriptions of the drillcore the mineralization is unlikely to respond to electromagnetic methods and does not appear to carry enough magnetite to be detected by magnetic methods.

7.2.4 Shihan Mineral Resource

Shihan is a zinc-rich VMS occurrence first mapped by Westfield Minerals in the 1960s. Mineralization is described as high-grade zinc with minor copper and lead, but also with significant gold and silver which are elevated in a separate nearby structure.

The mineralization is located within a steeply dipping east-west striking structure that is located approximately 400 south of a regional conductive trend. Interestingly the conductive trend to the north is very poorly developed along a strike distance parallel to the south-located Shihan mineralization. This suggests that the Shihan trend is related to the formational conductor to the north. The central location of Shihan is 726,780 mE and 5,367,020 mN.

The geology at Shihan is highly variable with massive conductive sulphide present, to thick sections of sphalerite with pyrite which should be a moderate conductor, to siliceous and argillaceous zones which are highly resistive.

7.3 INTERPRETATION OF 2020-02-17 SURVEY BLOCKS

Geophysical interpretation is focussed on the four survey blocks flown by BECI (East, South, West1, and West2) and then is expanded to previous surveys (Dighem, AeroTEM, and VTEM). Each survey block is summarised along with a list of identified conductor trends and their summarised interpretation. Conductor trends are primarily identified as formational conductors, or discrete conductors (VMS or gold targets). Formational conductors are typically interpreted as larger in scale with strike lengths of greater than 600m and can be conductive and/or have magnetic signal association. VMS targets tend to have good conductance (over 40% of signal remains at end of on-time signal decay) and can have magnetic signal association. Gold targets typically have no conductivity or magnetic signal association; however, it has been noted that gold zones within the Goudreau region tend to occur near weakly defined electromagnetic trends (non-formational) that are either sub-parallel or intersecting at 120° and/or 60° to formational trends. With the information provided it is not possible to effectively differentiate between formational and discrete conductive trends. The trends summarised may be interpreted as formational and/or discrete conductors.

7.3.1 East Block

Within the east survey block are 165°/345° striking thin dyke like structures that appear to be truncated by a large-scale formational trends locally striking north-east (35°) at the northern edge of the block. Three primary conductors have been identified within the east block and are presented in Figure 23 overlaying the early off-time EM response:

1. Along the western edge of the block a north-east trending conductor, striking approximately 20°/200°, is observed and appears to continue through the northeastern section of the south block. North-west striking electromagnetic conductors are identified in the southwestern region of the block and appear to continue through part of the south block as well.

2. The most southwestern conductor is at least 2 km long.

3. Running parallel to this trend is a set of conductive trends that are subparallel and appear to radiate outward from one another. Both trends are at least 6 km in length and appear to intersect the north-east trending conductor. These trends do not appear to have significant magnetic response but do appear to run parallel to magnetic susceptible structures. Each of these primary conductors have discontinuities potentially due to shear faulting.

Individual conductor trends and their potential target types are individually summarised in the supplementary ‘airtem-east-trends.csv’ file. Potential gold targets have primarily been identified along the northern north-east striking conductor trend (1) as well as the western edge of the set of subparallel conductor trends (3). Possible VMS targets have also been identified at the northern and southern limits of the set of subparallel conductor trends (3), these regions appear to have moderate to good conductance values in comparison with more central regions of the trends. Possible VMS targets have also been identified at the northern and southern limits of the set of subparallel conductor trends (3), these regions appear to have moderate to good conductance values in comparison with more central regions of the trends. Example electromagnetic responses along four different flight lines crossing gold (E-02, E-03, E-07, E-10, E-11, and E-19) and VMS conductor trends (E-10, E-11, and E-17) are shown in Figure 24. Primarily later time (orange and red) lines are decayed to background levels for the non-VMS, less conductive, targets. Lines were selected to present representative conductors in each region of the block. Conductors E-02 and E-03 appear to be dipping northwest. E-10, and E-11 appear to be dipping southwest. E-07 appears sub-vertical. E-17 and E-19 appear to dip west.

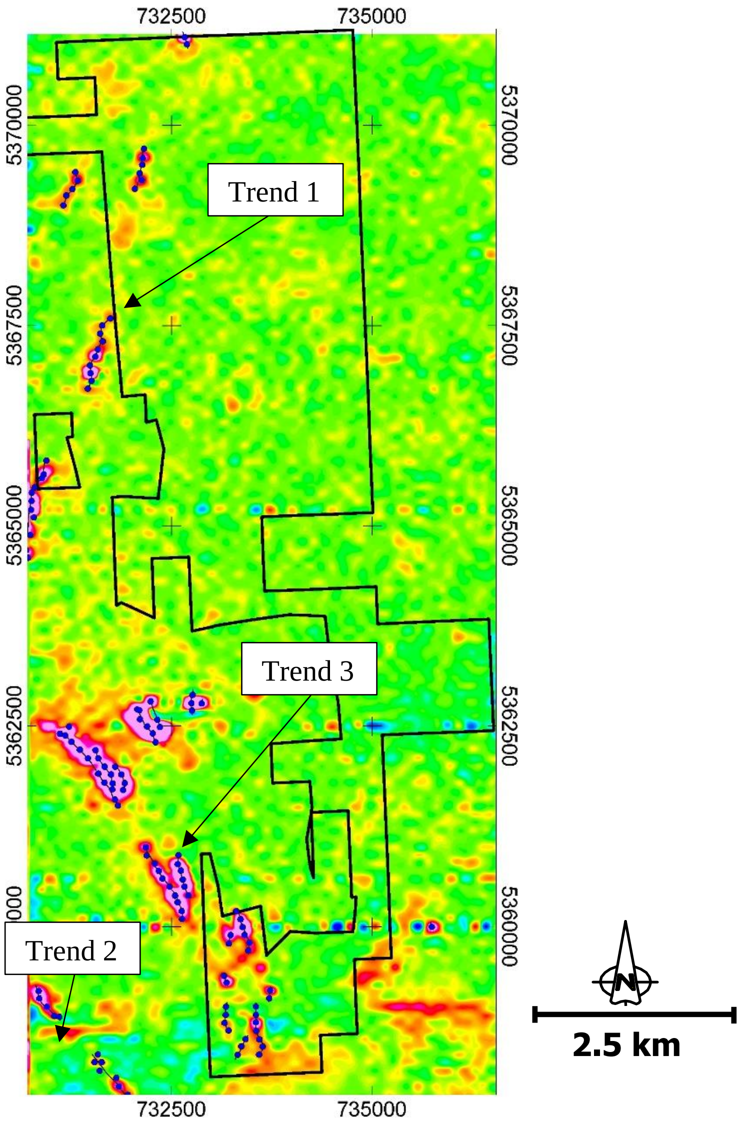

Figure 23 – East block EM response (zOff[0]). Conductor trends are marked in blue. Projected in NAD83 / UTM Zone 16N.

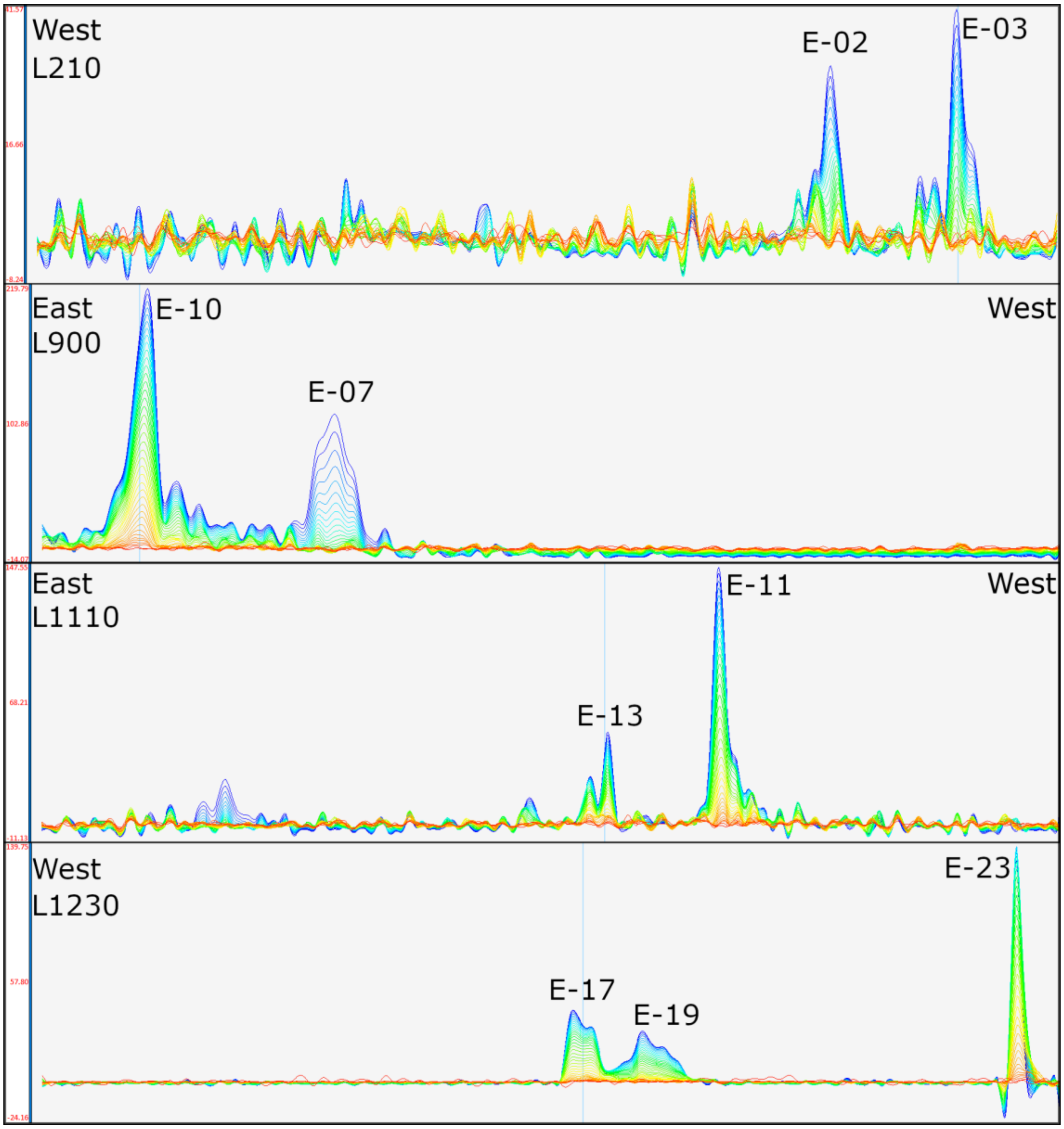

Figure 24 – Four line profiles showing example conductive trends for the east block. East and West labels eastward or westward end of the line, respectively.

7.3.2 South Block

Within the south survey block are thin dyke like structures striking at 105°/285°-130°/310°. The western edge of the survey block shows evidence of dykes striking at approximately 150°/330° with nearly perpendicularly intersecting dykes striking at 55°/235°. The Stover property is located northeast of a northwest trending magnetic and electromagnetic responsive structure. Conductor trends have been identified trending parallel and subparallel to this structure and are presented in Figure 25 with the early off-time EM response.

Individual conductor trends and their potential target types are individually summarised in the supplementary 'airtem-south-trends.csv' file. Conductor trends were primarily identified in the central region of the south block, running parallel with the strong magnetic structure (striking approximately 120°/300°), and along the eastern edge of the south block, striking east-west (90°/270°). Example electromagnetic responses along four different flight lines crossing gold (S-18, S-26, S-27, S-28,S-42, S-43, S-44, S-45, and S-46) and a VMS conductor trend (S-04) are shown in Figure 26. Primarily later time (orange and red) lines are decayed to background levels for the non-VMS, less conductive, targets. Primarily later time (orange and red) lines are decayed to background levels for the non-VMS, less conductive, targets. Lines were selected to present representative conductors in each region of the block. Conductors S-42 through S-46 are difficult to determine dip direction due to the complexity of the EM response, but potentially south. Conductors S-26 to S-28 are also difficult to determine dipping direction, but potentially sub-vertical to southeast. S-11, S-18 and S-20 appear to be dipping southwest. S-04 appears to be dipping northeast. S-03 appears near vertical to northeast.

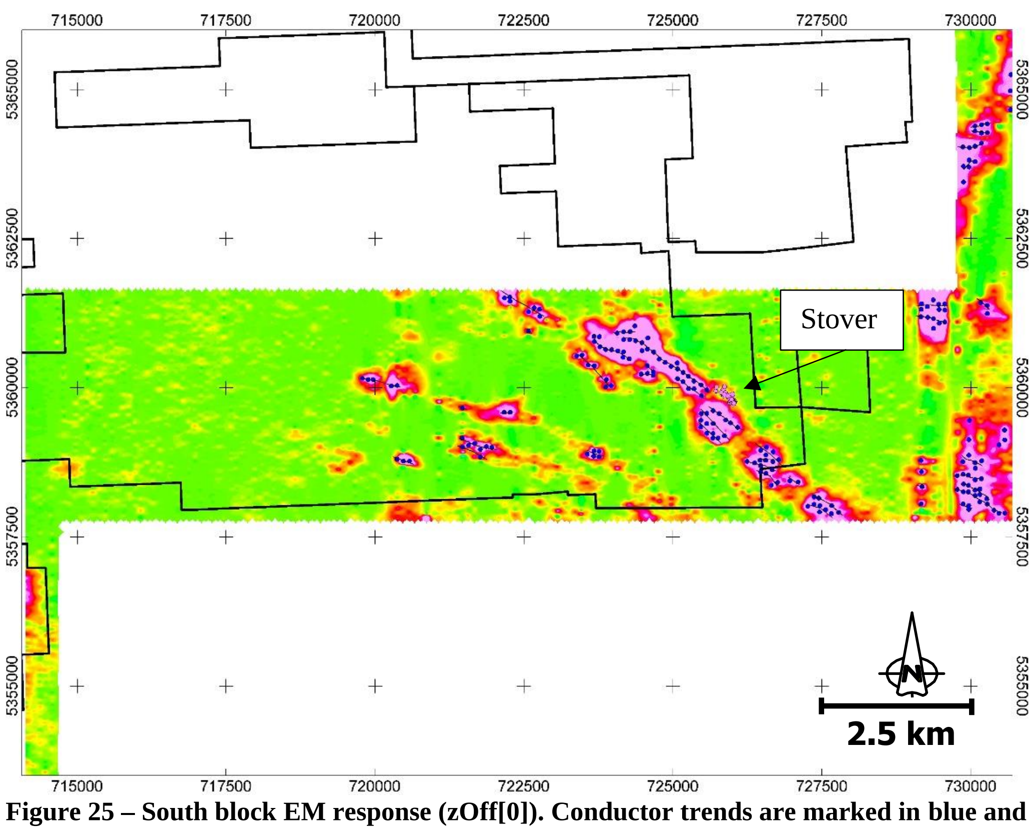

Figure 25 – South block EM response (zOff[0]). Conductor trends are marked in blue and the Stover Prospect drill collars are marked in magenta. The Goudreau property outlined in black. Projected in NAD83 / UTM Zone 16N.

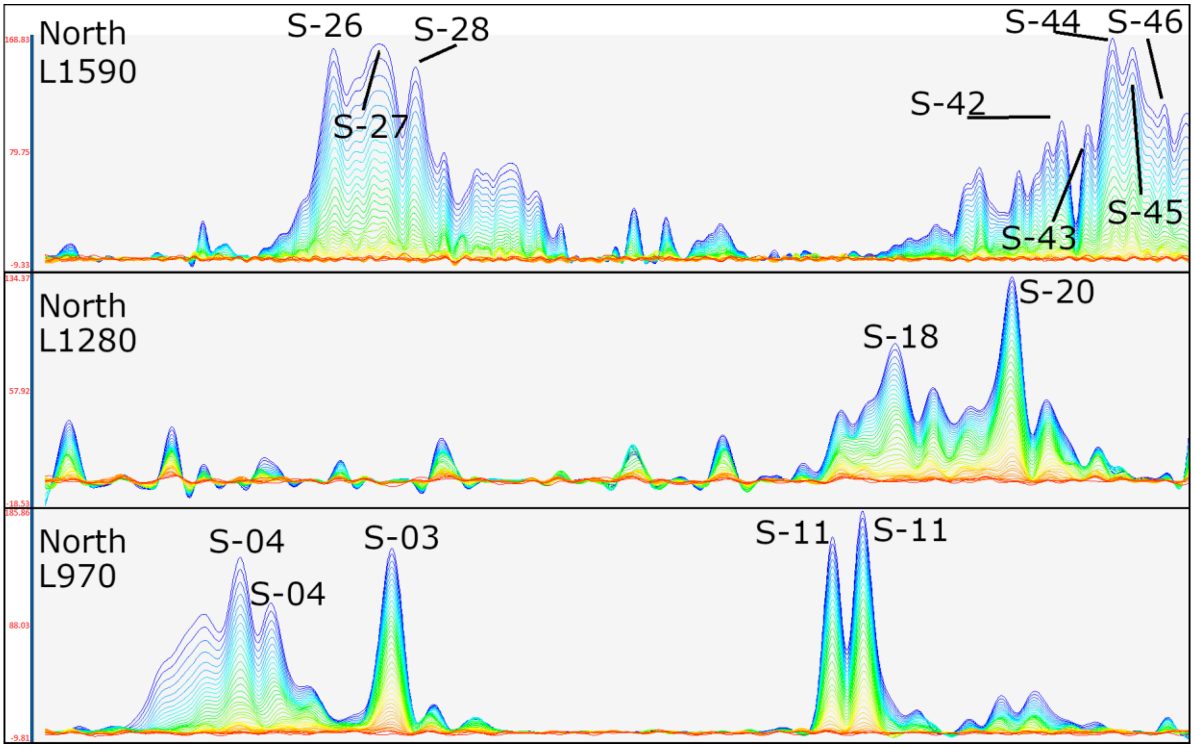

Figure 26 – Three line profiles showing example conductive trends for South block. North label indicates northern end of survey line.

7.3.3 West1 Block

Within the west1 survey block are magnetically susceptible structures striking at orientations similar to those mentioned for the east and south bocks. Within the north and west regions of the west1 block are magnetic trends striking east-west (90°/270°) and northwest (150°/330°) and within the southeastern region magnetic trends are striking northeast (35°/215°). Five major conductive trends, presented in Figure 27 overlaying early off-time EM response, have been identified and tend to run parallel or sub-parallel to these magnetic structures. Overall trends appear to extend from 200 m to over 3 km.

Individual conductor trends and their potential target types are individually summarised in the supplementary 'airtem-west1-trends.csv' file. Conductor trends were primarily identified in the regions mentioned above, running parallel with the magnetic structures (striking approximately 120°/300°). Example electromagnetic responses along two different flight lines (L180 and L1080) crossing gold (W-07, W-24, W-41, W-44, W-46, and W-47) and a VMS conductor trend (W-01, W-02, W-14, W-18, W-21, and W-24) are shown in Figure 28. Primarily later time (orange and red) lines are decayed to background levels for the non-VMS, less conductive, targets. Lines were selected to present representative conductors in each region of the block. Conductors W-01, W-02, and W-14 appear to be steeply dipping south. Conductor W-07 appears to be dipping southwest. Conductors W-18, W-21, and W-24 appear to be dipping near vertical. Conductors W-41, W-44, W-47, and W-46 appear to be steeply dipping northwest.

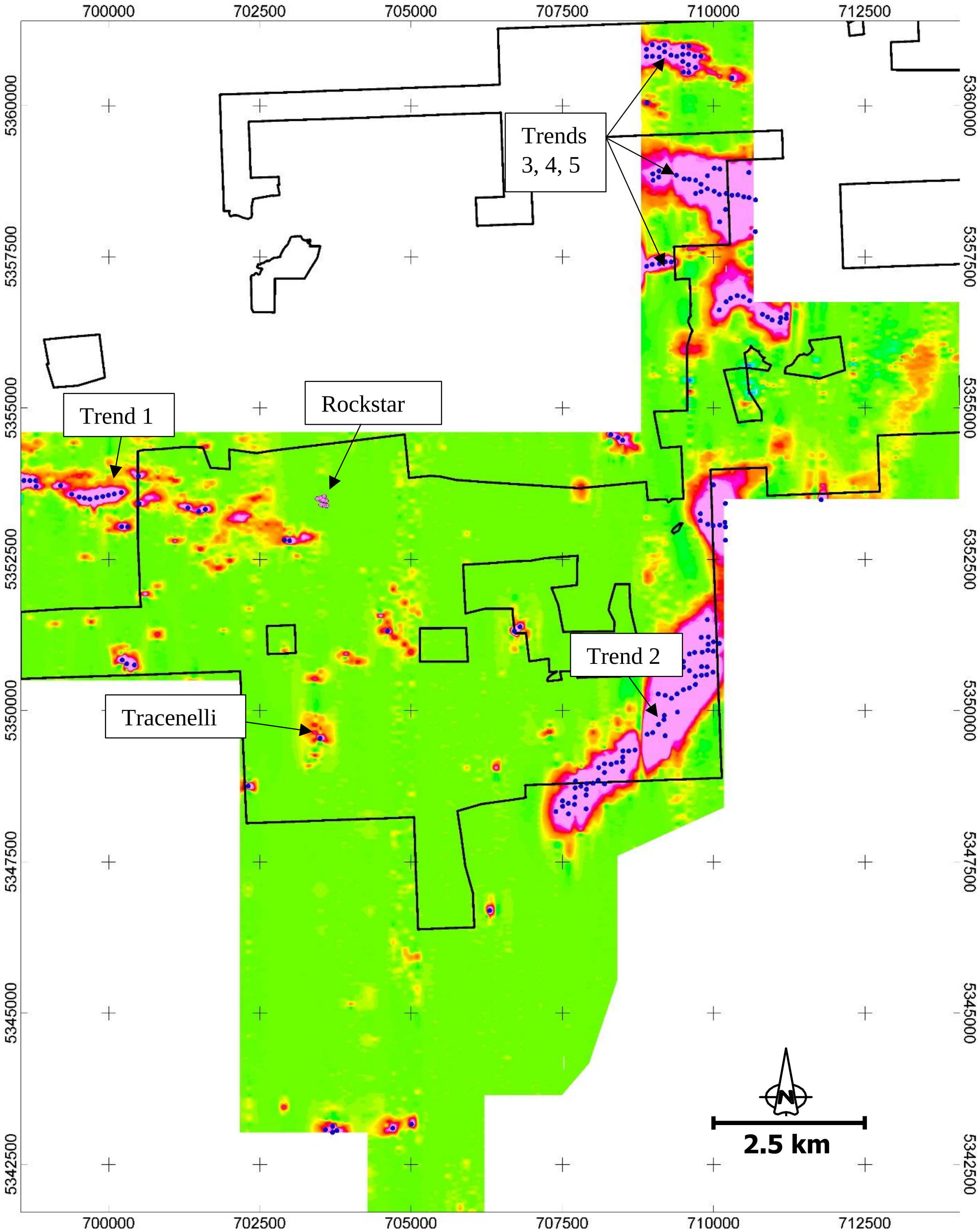

Figure 27 – West1 block EM response (zOff[0]). Conductor trends are marked in blue and the Rockstar Prospect drill collars are marked in magenta. The Goudreau property outlined in black. Projected in NAD83 / UTM Zone 16N.

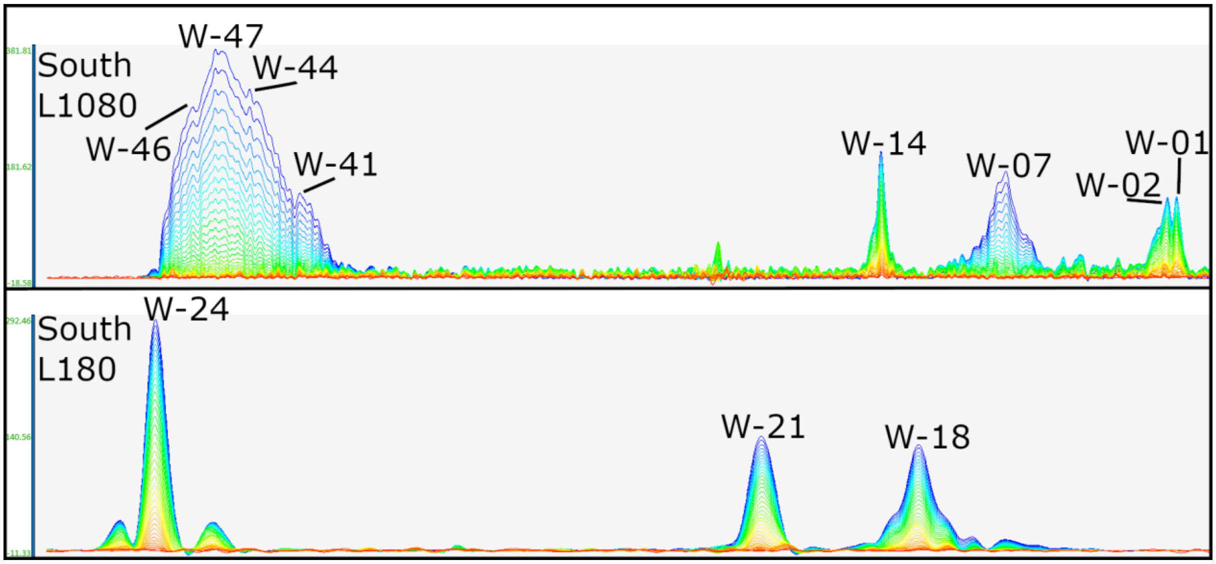

Figure 28 - Two line profiles showing example conductive trends for West1 block. South label indicates southern end of survey line.

7.3.4 West2 Block

Within the west2 survey block are magnetically susceptible structures striking at 90°/270° and 165°/345°. Conductive trends have been identified, presented in Figure 29 with the early off-time EM response, and are primarily east-west trending and appear to be related to trends identified in the west1 block. Overall trends appear to extend from 700 m to over 1.5 km.

Individual conductor trends and their potential target types are individually summarised in the supplementary 'airtem-west2-trends.csv' file. Conductor trends primarily strike in an east-west direction and appear to intersect the 165°/345° magnetic structures and run subparallel with the 90°/270° structures. Example electromagnetic responses along two different flight lines (L110 and L280) crossing gold (W2-04, and W2-05) and a VMS conductor trends (W2-01, and W2-02) are shown in Figure 30. Primarily later time (orange and red) lines are decayed to background levels for the non-VMS, less conductive, targets. Lines were selected to present representative conductors in each region of the block. Conductors W2-01 and W2-05 appears to dip south. W2-02, W2-03, and W2-04 appear to be near vertical.

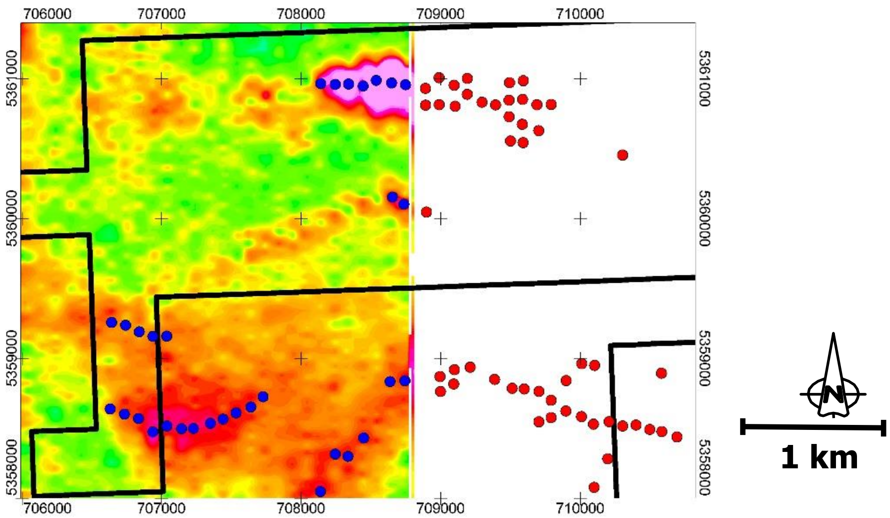

Figure 29 – West2 block EM response (zOff[0]). West2 conductor trends are marked in blue and West1 conductor trends are marked in red. The Goudreau property outlined in black. Projected in NAD83 / UTM Zone 16N.

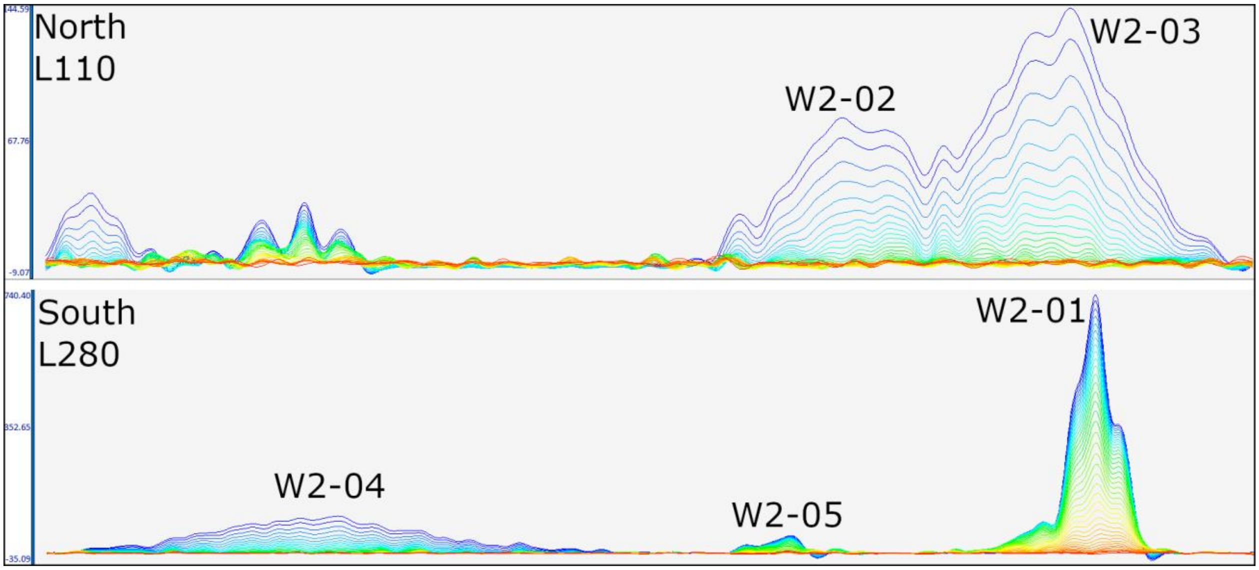

Figure 30 - Two line profiles showing example conductive trends for West2 block. South and North labels indicate southern and northern end of survey line, respectively.

7.4 INTERPRETATION OF PREVIOUS SURVEY WORK

7.4.1 Dighem

The Dighem system is a helicopter-borne magnetic and frequency domain electromagnetic system. It offers good lateral resolution (10s of meters) and moderate depth penetration (100 m). There are two coil configurations, coaxial (CX) and coplanar (CP). The coaxial coils highlight steeply dipping conductors and operate at two frequencies (900 and 7,200 Hz). The coplanar coils better energize flat-lying and/or thick conductors and operate at two frequencies (900 and 7,200 Hz). The higher frequency better energizes poor conductors but can be sensitive to conductive overburden. The lower frequency offers better depth penetration, detects higher conductance targets but has higher noise levels (compared to the low frequency). The Dighem coplanar 900 Hz results are presented in Figure 31 (full survey area) and in Figure 32 (Goudreau property).

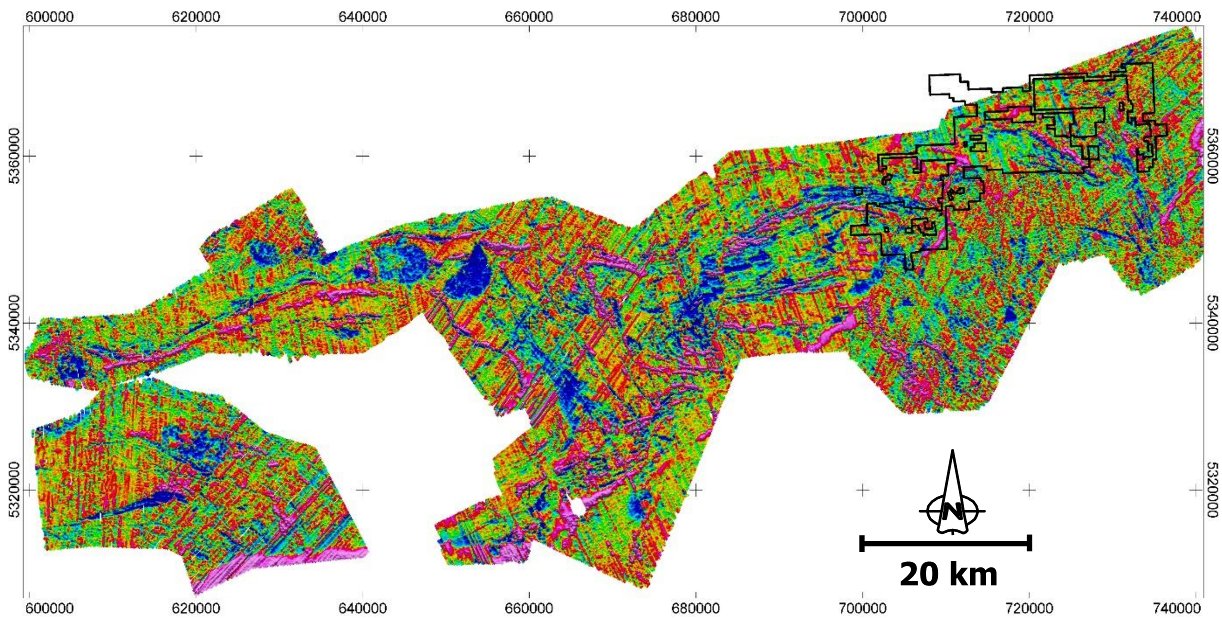

Figure 31 – Dighem 1988 survey results (CPI900) with Goudreau survey property outline in black. Projected in NAD83 / UTM Zone 16N.

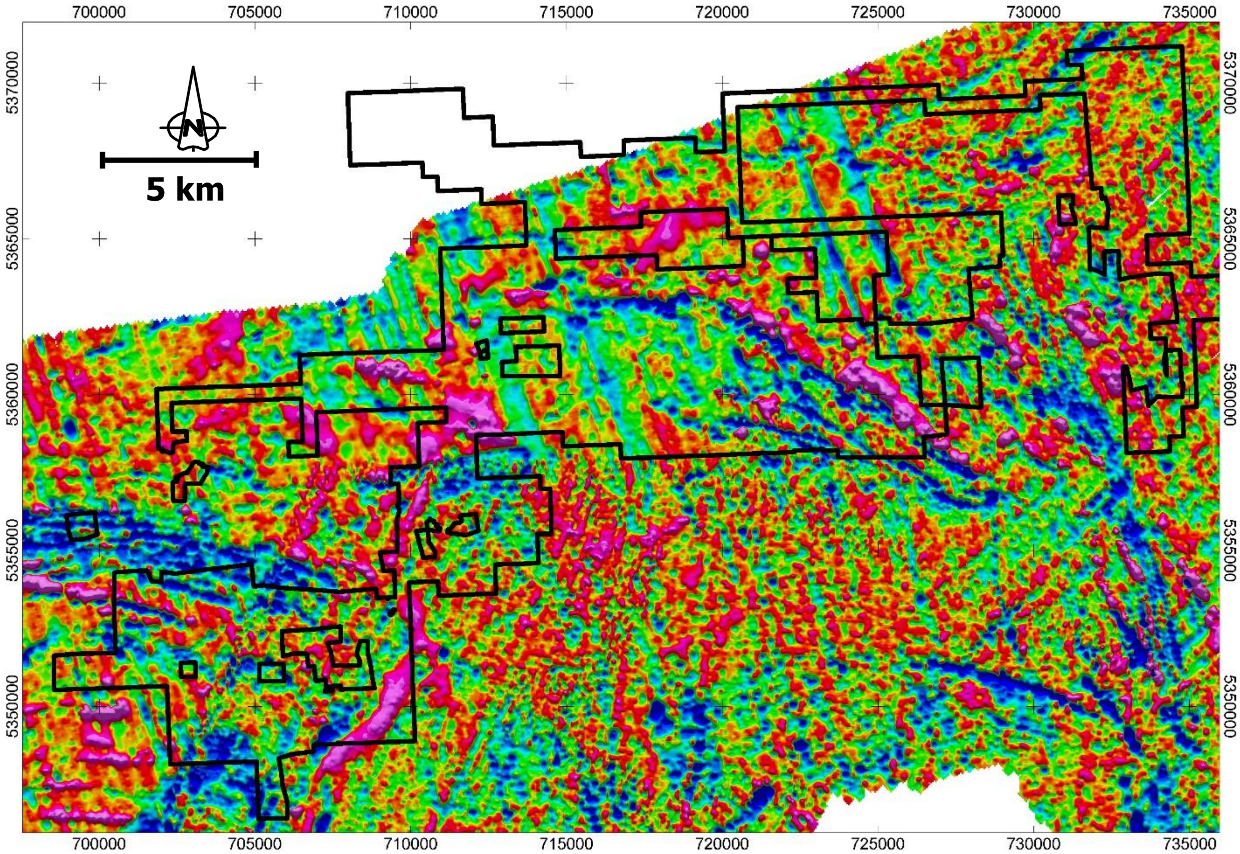

Figure 32 - Dighem 1988 survey results (CPI900) over Goudreau property (outlined in black). Projected in NAD83 / UTM Zone 16N.

7.4.1.1 Dighem Results Stover

The Dighem CP coil in-phase response for the 900 Hz base frequency (CPI900) is shown in Figure 33 for the area around the Stover drilling (as indicated by arrow). Drill collars are shown in magenta. The mineralization is not identified by either the EM or magnetic response. But there is a northwest trending response that appears to terminate along a contact that correlates strongly with the Stover Prospect. Further to the northwest this trend is identified as a formational conductor (blue symbols) from the VTEM survey. A review of the CX coil responses suggests a steeply dipping conductor of variable thickness. In the area around Stover the conductor has sufficient thickness to appear as a flat-lying conductor (CP response is greater than the CX response). A north-south (interpreted) fault appears to terminate the Stover mineralization to the west. But the conductive trend continues to the west suggesting mineralization could continue in that direction as well, possibly offset.

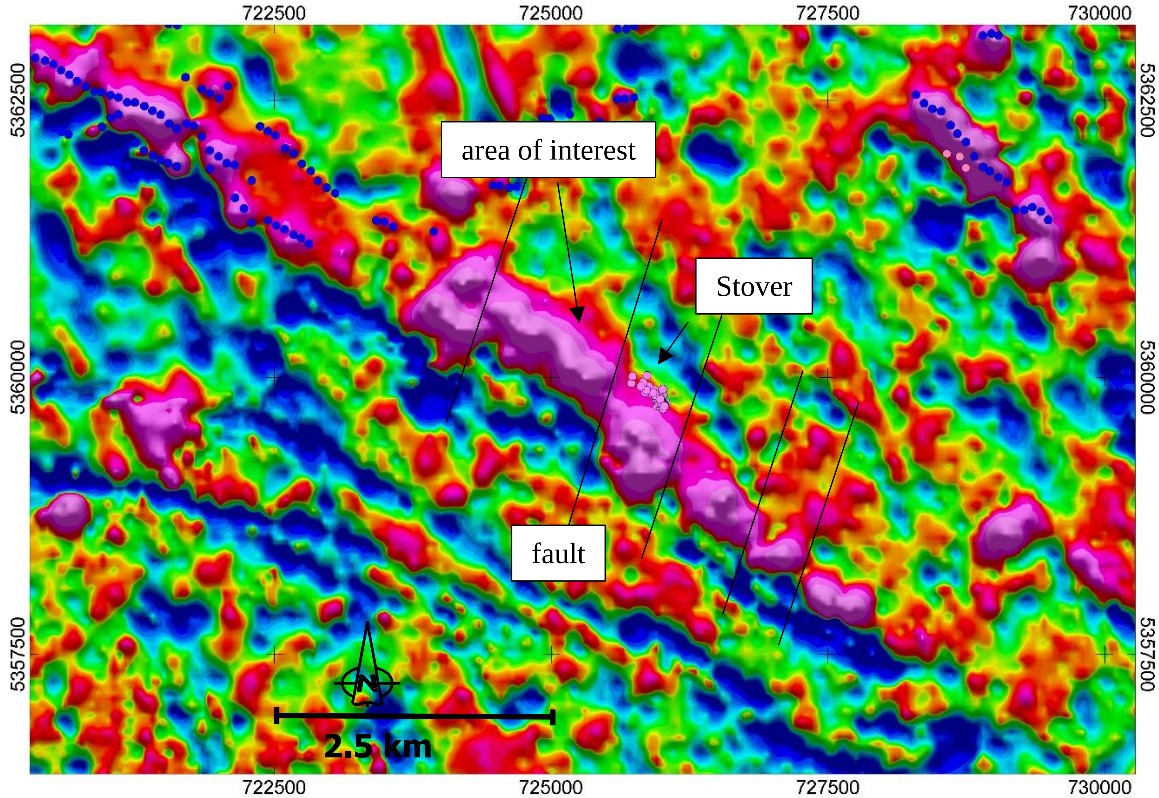

Figure 33 - Dighem CPI900 response over the Stover Prospect. Projected in NAD83 / UTM Zone 16N.

7.4.1.2 Dighem Results Rockstar

The Dighem CP coil in-phase response for the 900 Hz base frequency (CPI900) is shown in Figure 34 for the area around the Rockstar region. Drill collars are shown in pink and West 1 conductor trends are shown in red. There is an east-west trending response that appears to correlate with the Rockstar drill collars. A review of the CP and CX coil responses suggests a dipping conductor of constant thickness. This conductive trend appears to continue with similar conductance westward suggesting mineralization could continue in that direction. To the east, a steeply dipping conductor (strong CX) trending northeast appears to crosscut the Rockstar trend where the Rockstar trend does not appear to continue afterwards.

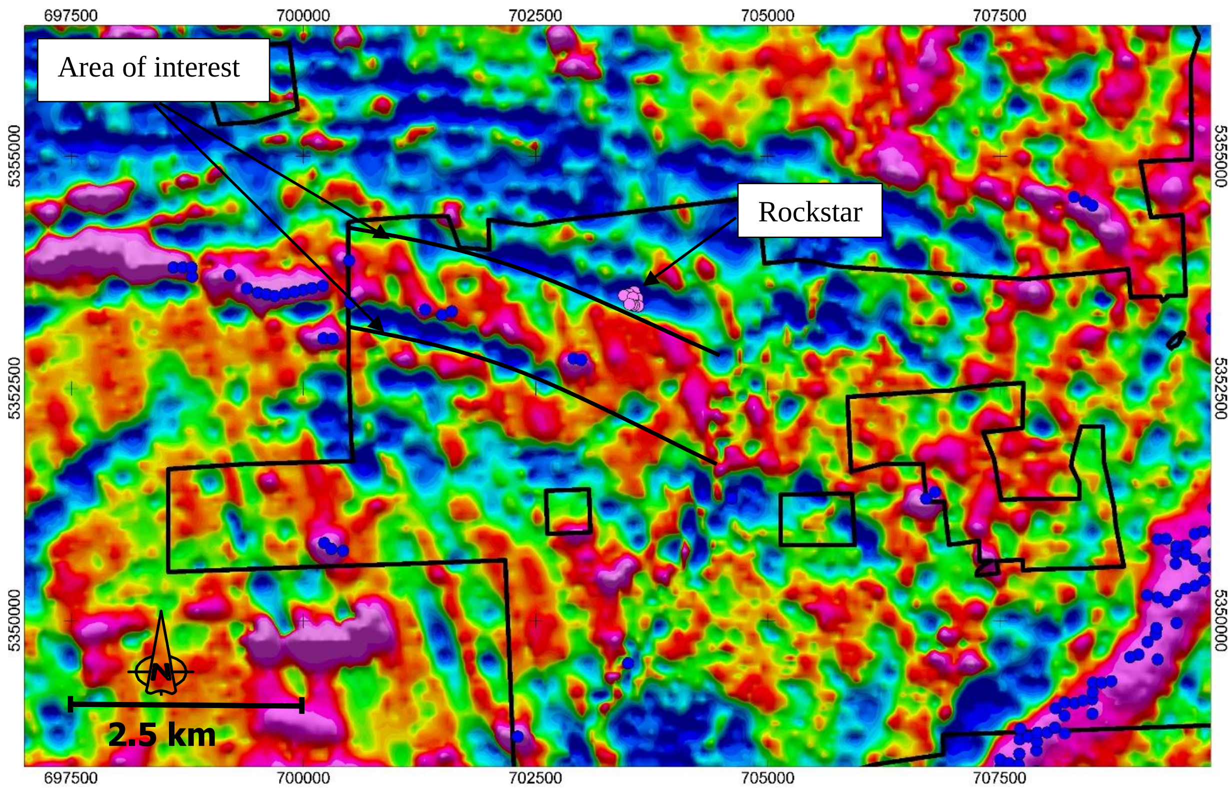

Figure 34 – Dighem CPI900 over Rockstar Prospect. Projected in NAD83 / UTM Zone 16N.

7.4.1.3 Dighem Results Tracenelli

The Dighem CP coil in-phase response for the 900 Hz base frequency (CPI900) is shown in Figure 35 for the area around the Tracenelli prospect. West 1 conductor trends are shown in red. A northeast trending steeply dipping conductor (strong CX) appears to cross the central Tracenelli region, which continues up east of the Rockstar region. A review of the CP and CX coil responses suggests there are east-west steeply dipping conductors to the west of the Goudreau property but terminate before the Tracenelli region.

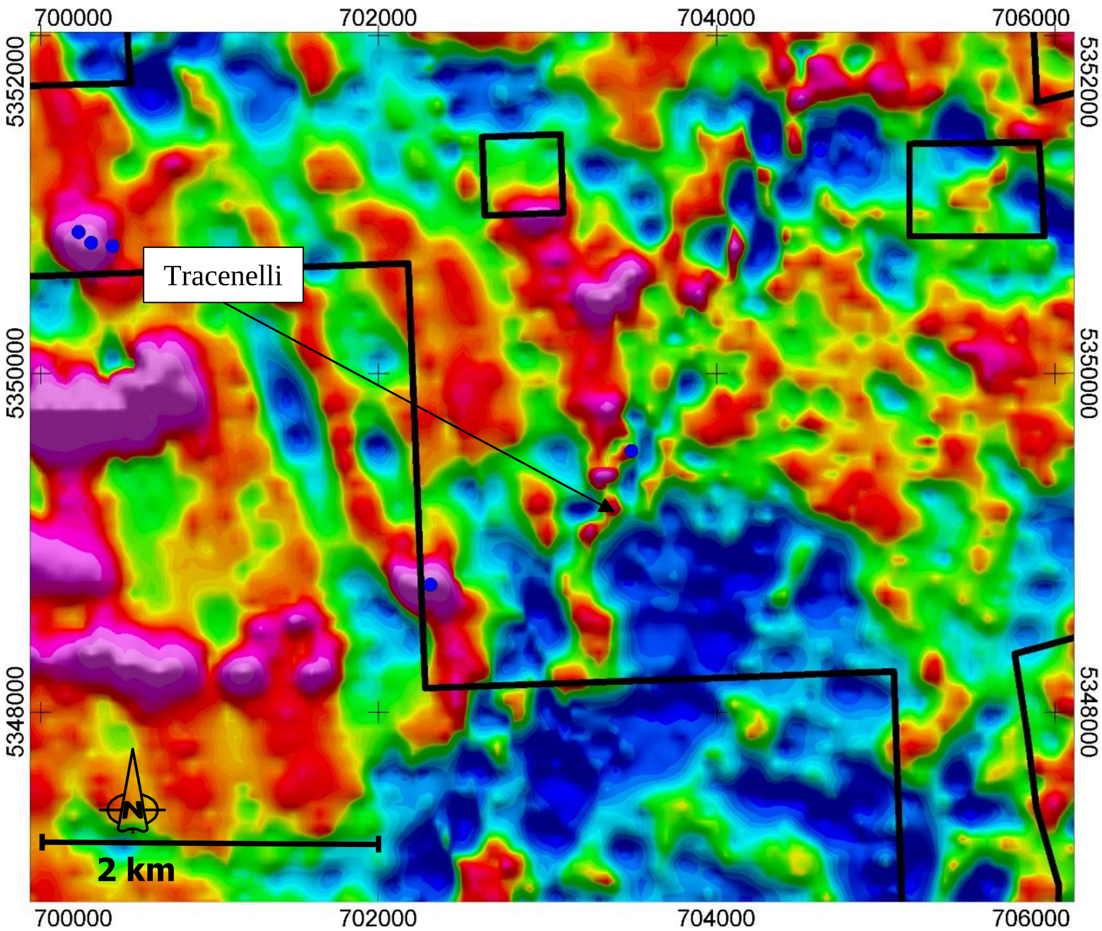

Figure 35 - Dighem CPI900 over Tracenelli Prospect. Projected in NAD83 / UTM Zone 16N.

7.4.1.4 Dighem Results Shihan

The Dighem CP coil in-phase response for the 900 Hz base frequency (CPI900) is shown in Figure 36 for the area around the Shihan drilling (as indicated by arrow). Drill collars are shown in magenta. There is a weak east-west trending response that appears to terminate east of Shihan Prospect. To the west this trend continues is identified as a formational conductor from the AeroTEM Magpie1 survey. The conductive trend continues to the west suggesting mineralization could continue in that direction as well, possibly offset.

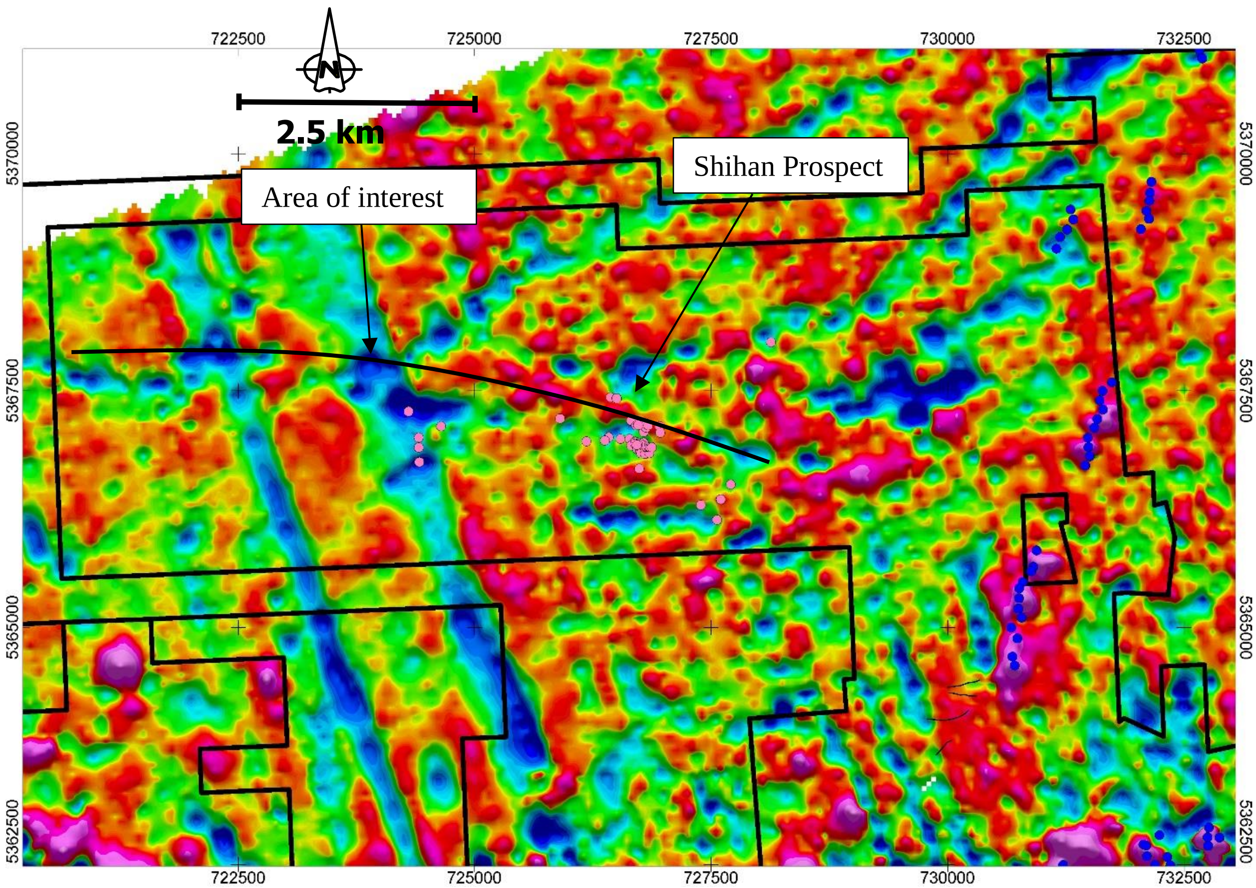

Figure 36 - Dighem CPI900 over Shihan Prospect. Projected in NAD83 / UTM Zone 16N.

7.4.2 VTEM

The VTEM survey highlights a large magnetic structure continuing from the South block into the central region of Magpie1. The structure is trending northwest and is folded to trend west. This structure appears to be dipping southwest to south. A strong formational conductor runs parallel to this magnetic structure. Discrete conductors are identified as subparallel trends offset from formational conductors and having lower conductance, both are presented with the early off-time EM response in Figure 37. The eastern edge of Magpie1 contains north-south (165°/345°) and northeast (60°/240°) trending dyke-like structures as well as east-west to northeast folded structures in the northeast. Formational conductors have been identified in this region as well and used to assist in identifying potential discrete conductor targets.

Individual discrete conductor trends are summarised in the supplementary 'vtem-magpie1-trends.csv' file. Conductor trends are primarily striking in an east-west to southeast direction and run parallel to formational trends. Example electromagnetic responses along four different flight lines (L1250, L1830, L2480, and L3450) crossing potential gold targets (M1-01, M1-05, M1-08, M1-10, M1-14, M1-15, and M1-23) are shown in Figure 38. These conductors are weaker in amplitude than the formational conductors with later time signal (orange and red lines) decayed to background levels. Lines were selected to present representative conductors in each region of the block. Conductor M1-01 is subvertical to dipping southwest. Conductor M1-05 is near vertical. M1-08, M1-10, M1-14, M1-15 and M1-23 all appear to be dipping steeply north to northeast.

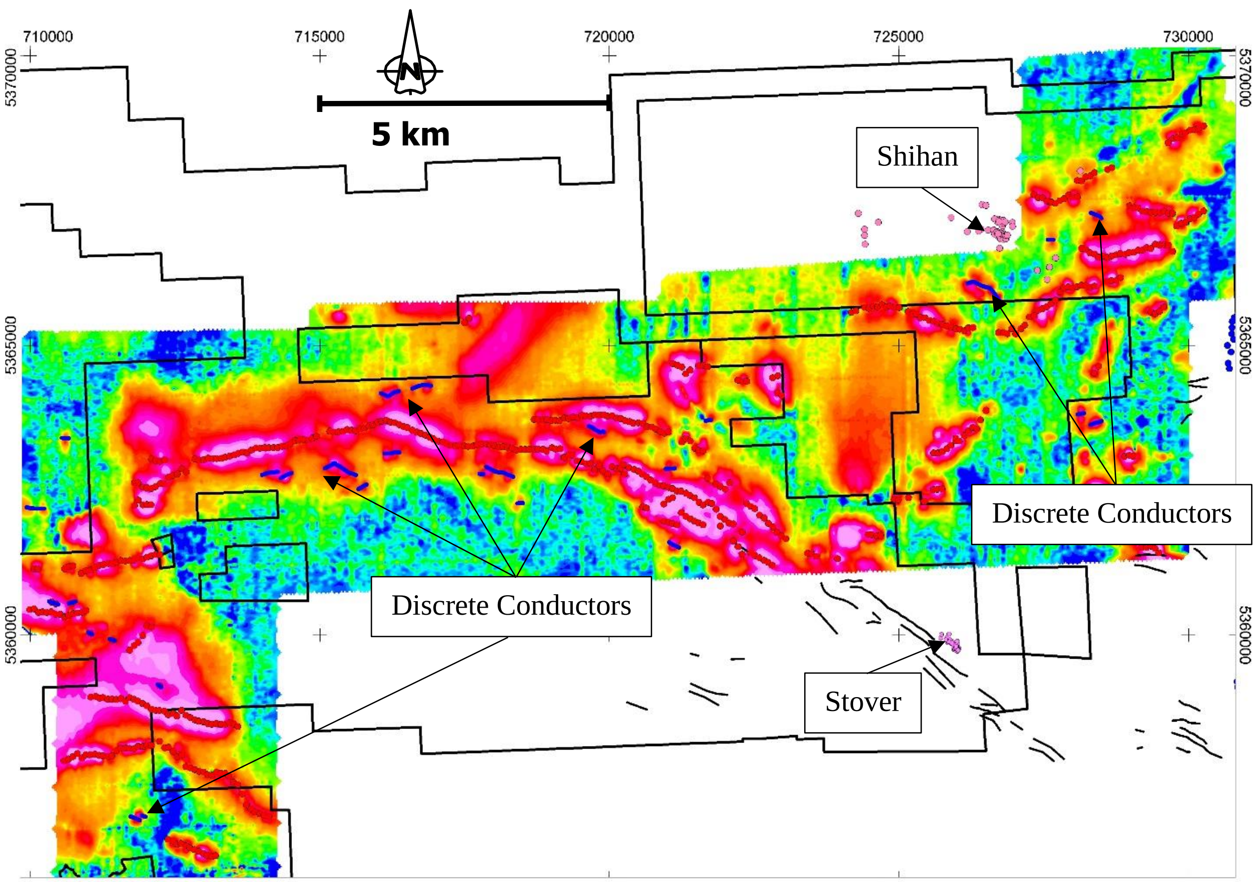

Figure 37 – Magpie1 VTEM block EM response (zOff[0]). Formational and discrete conductor trends are marked in red and blue, respectively. The Goudreau property outlined in black. Projected in NAD83 / UTM Zone 16N.

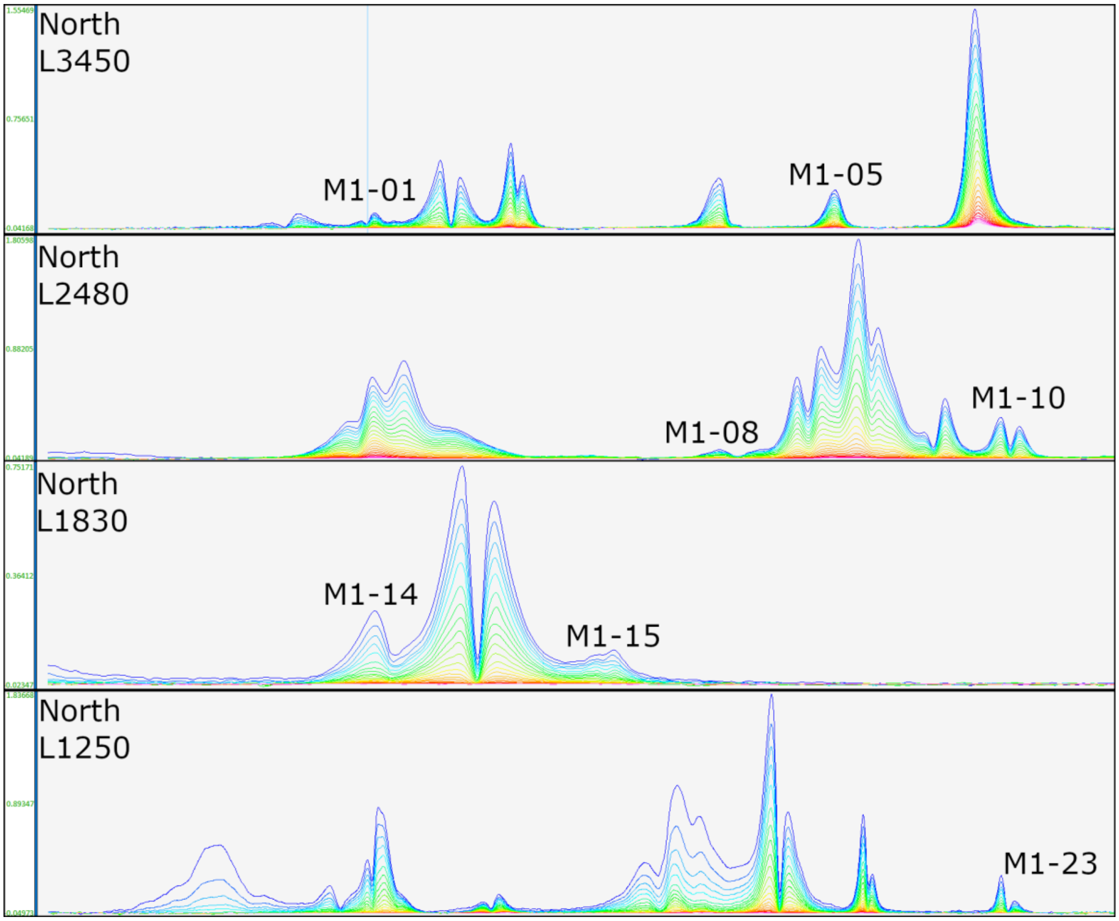

Figure 38 - Four line profiles showing example conductive trends for Magpie1 block. North label indicates northern end of survey line.

7.4.3 AeroTEM Shihan Ridgeline

The AeroTEM Shihan Ridgeline TMI and early off-time (zoff[0]) are shown in Figure 39 with formational and discrete conductors marked with red and blue circles, respectively. Within the Shihan survey block are magnetically susceptible structures striking at 90°/270° and 165°/345°. Conductive trends have been identified and are primarily east-west trending. A linear magnetic structure trending northeast (55°) appears to coincide with a southeastern conductive unit.

Individual conductor trends and their potential target types are listed and summarized in the supplementary 'aerotem-shihan-ridgeline-trends.csv' file. Conductor trends primarily strike in an east-west direction but range between northeast and southeast. Most appear to run subparallel to magnetic structures and coincide with locations that present evidence of faulting and/or folding. Example electromagnetic responses along three different flight lines (L10040, L11460, and L11790) crossing gold target (Sh-02, Sh-06, and Sh-10) are shown in Figure 40. Primarily later time channels are decayed to background levels. Lines were selected to present representative conductors in each region of the block. Conductors Sh-02 and Sh-06 appear to dip south. Sh-10 appear to be near vertical.

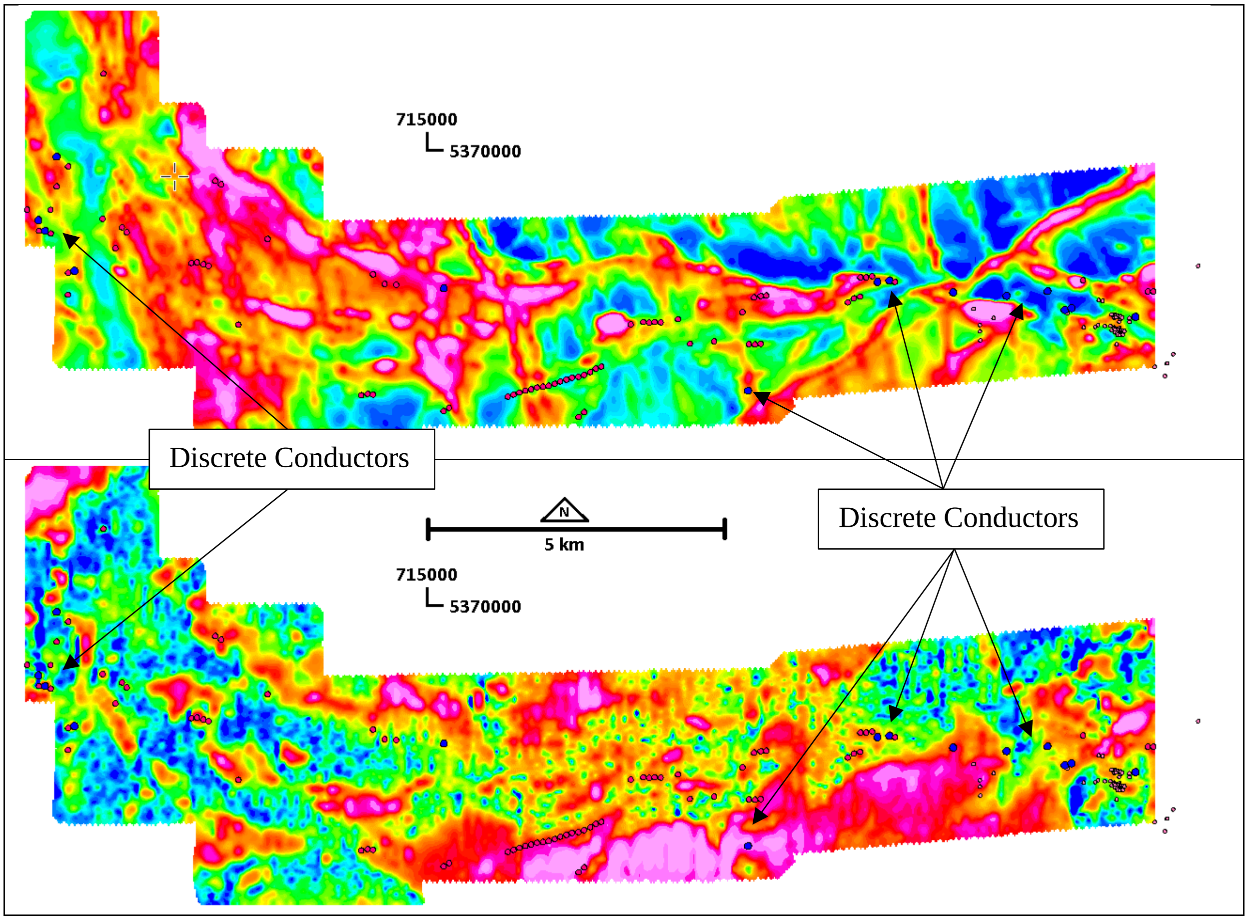

Figure 39 – AeroTEM Shihan Ridgeline survey results showing TMI (top) and early off-time (Zoff[0]) (bottom). Red circles are formational trends. Blue circles are discrete trends summarized in supplementary material. Projected in NAD83 / UTM Zone 16N.

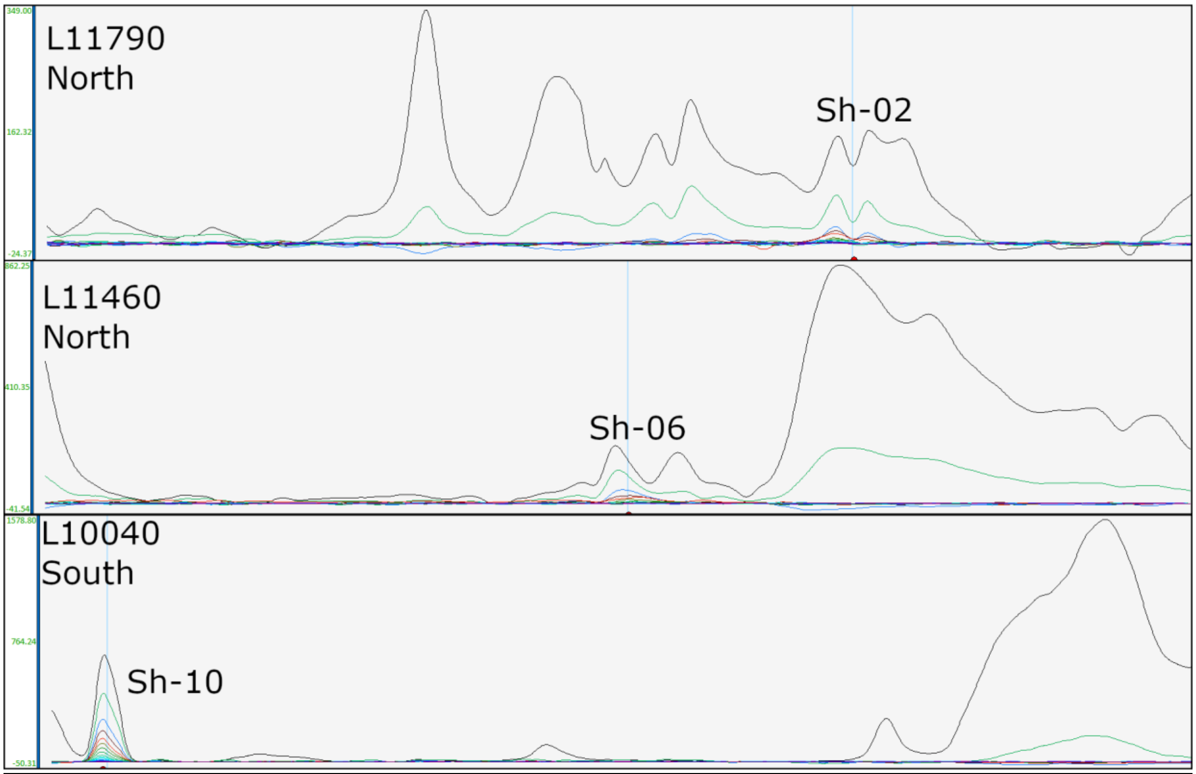

Figure 40 - Three line profiles showing example conductive trends for Shihan Ridgeline block. South and North labels indicate the southern and northern end of survey line, respectively.

8.0 QUALIFICATIONS

I, Michael Cunningham, do hereby claim the following to be true:

1. I am a professional geoscientist (P.Geo.) in good standing, registered with the Association of Geoscientists of Ontario (#3007);

2. I am a graduate of Carleton University with a degree in Earth Sciences (Geophysics) (M.Sc, 2016);

3. I am a practicing exploration geophysicist with more than 5 years experience and reside at F-3070 Councillor's Way, Ottawa, Ontario, K1T 2S6;

4. I have no direct interest in the Goudreau Project property or in Manitou Resources Ltd.;

5. I prepared this report and I am solely responsible for its contents.

Dated at Ottawa, Ontario on the 1st day of October 2020.

Michael Cunningham, P.Geo.
Geophysicist
Balch Exploration Consulting Inc.

APPENDIX A – OUTLINE OF SURVEY POLYGONS

Table 6, Table 7, Table 8 and Table 9 shows the polygon corners in meters easting and northing, NAD-83 and UTM ZONE 16nN.

Table 6 – Corner coordinates for the East survey block.

East NAD-83	
Easting (m)	**Northing (m)**
730700.2	5371200.4
736550.6	5371200.8
736550.9	5357900.2
730700.4	5357900.5

Table 7 – Corner coordinates for the South survey block.

South NAD-83	
Easting (m)	**Northing (m)**
714070.7	5361500.2
729830.9	5361500.6
729830.0	5366000.0
730700.0	5366000.0
730700.1	5357900.1
714610.2	5357900.1
714611.0	5353500.8
714070.0	5353500.5

Table 8 – Corner coordinates for the West-1 survey block.

West-1 NAD-83	
Easting (m)	**Northing (m)**
698550.6	5350500.2
702170.6	5350500.7
702170.1	5348247.5
702170.0	5343030.0
704280.0	5343030.0
704280.0	5341710.0
706210.0	5341710.0
706210.0	5343650.0
707495.0	5343650.0
707940.0	5344170.0
708410.0	5345555.0
708410.0	5347600.0
710170.0	5348400.0
710170.2	5353500.5
714070.9	5353500.0
714070.9	5356750.7
710660.4	5356750.2
710660.5	5361400.5
708800.9	5361400.0
708800.8	5354600.2
698550.1	5354600.6

Table 9 – Corner coordinates for the West-2 survey block.

West-2 NAD-83	
Easting (m)	**Northing (m)**
705990.5	5358000.7
705990.8	5361400.8
708811.0	5361400.1
708811.0	5358000.4